

UNCLASSIFIED

AD NUMBER
ADB275663
NEW LIMITATION CHANGE
TO Approved for public release, distribution unlimited
FROM Distribution authorized to U.S. Gov't. agencies only; Proprietary Info.; Oct 2001. Other requests shall be referred to U.S. Army Medical Research and Materiel Command, 504 Scott St., Ft. Detrick, MD 21702-5012.
AUTHORITY
USAMRMC ltr, 28 Aug 2002

THIS PAGE IS UNCLASSIFIED

AD _____

Award Number: DAMD17-98-1-8617

TITLE: Role of Glutamate Release and Metabotropic Autoreceptors
in Seizureogenic Actions of Cholinomimetic Agents

PRINCIPAL INVESTIGATOR: Thomas W. Vickroy, Ph.D.

CONTRACTING ORGANIZATION: The University of Florida
Gainesville, Florida 32611-5500

REPORT DATE: October 2001

TYPE OF REPORT: Final

PREPARED FOR: U.S. Army Medical Research and Materiel Command
Fort Detrick, Maryland 21702-5012

DISTRIBUTION STATEMENT: Distribution authorized to U.S. Government
agencies only (proprietary information, Oct 01). Other requests
for this document shall be referred to U.S. Army Medical Research
and Materiel Command, 504 Scott Street, Fort Detrick, Maryland
21702-5012.

The views, opinions and/or findings contained in this report are
those of the author(s) and should not be construed as an official
Department of the Army position, policy or decision unless so
designated by other documentation.

20020225 076

NOTICE

USING GOVERNMENT DRAWINGS, SPECIFICATIONS, OR OTHER DATA INCLUDED IN THIS DOCUMENT FOR ANY PURPOSE OTHER THAN GOVERNMENT PROCUREMENT DOES NOT IN ANY WAY OBLIGATE THE U.S. GOVERNMENT. THE FACT THAT THE GOVERNMENT FORMULATED OR SUPPLIED THE DRAWINGS, SPECIFICATIONS, OR OTHER DATA DOES NOT LICENSE THE HOLDER OR ANY OTHER PERSON OR CORPORATION; OR CONVEY ANY RIGHTS OR PERMISSION TO MANUFACTURE, USE, OR SELL ANY PATENTED INVENTION THAT MAY RELATE TO THEM.

LIMITED RIGHTS LEGEND

Award Number: DAMD17-98-1-8617
Organization: The University of Florida

Those portions of the technical data contained in this report marked as limited rights data shall not, without the written permission of the above contractor, be (a) released or disclosed outside the government, (b) used by the Government for manufacture or, in the case of computer software documentation, for preparing the same or similar computer software, or (c) used by a party other than the Government, except that the Government may release or disclose technical data to persons outside the Government, or permit the use of technical data by such persons, if (i) such release, disclosure, or use is necessary for emergency repair or overhaul or (ii) is a release or disclosure of technical data (other than detailed manufacturing or process data) to, or use of such data by, a foreign government that is in the interest of the Government and is required for evaluational or informational purposes, provided in either case that such release, disclosure or use is made subject to a prohibition that the person to whom the data is released or disclosed may not further use, release or disclose such data, and the contractor or subcontractor or subcontractor asserting the restriction is notified of such release, disclosure or use. This legend, together with the indications of the portions of this data which are subject to such limitations, shall be included on any reproduction hereof which includes any part of the portions subject to such limitations.

THIS TECHNICAL REPORT HAS BEEN REVIEWED AND IS APPROVED FOR PUBLICATION.

REPORT DOCUMENTATION PAGE

Form Approved
OMB No. 074-0188

Public reporting burden for this collection of information is estimated to average 1 hour per response, including the time for reviewing instructions, searching existing data sources, gathering and maintaining the data needed, and completing and reviewing this collection of information. Send comments regarding this burden estimate or any other aspect of this collection of information, including suggestions for reducing this burden to Washington Headquarters Services, Directorate for Information Operations and Reports, 1215 Jefferson Davis Highway, Suite 1204, Arlington, VA 22202-4302, and to the Office of Management and Budget, Paperwork Reduction Project (0704-0188), Washington, DC 20503

1. AGENCY USE ONLY (Leave blank)	2. REPORT DATE October 2001	3. REPORT TYPE AND DATES COVERED Final (1 Oct 98 - 30 Sep 01)	
4. TITLE AND SUBTITLE Role of Glutamate Release and Metabotropic Autoreceptors in Seizuregenic Actions of Cholinomimetic Agents		5. FUNDING NUMBERS DAMD17-98-1-8617	
6. AUTHOR(S) Thomas W. Vickroy, Ph.D.			
7. PERFORMING ORGANIZATION NAME(S) AND ADDRESS(ES) The University of Florida Gainesville, Florida 32611-5500 E-mail: vickroy@ufl.edu		8. PERFORMING ORGANIZATION REPORT NUMBER	
9. SPONSORING / MONITORING AGENCY NAME(S) AND ADDRESS(ES) U.S. Army Medical Research and Materiel Command Fort Detrick, Maryland 21702-5012		10. SPONSORING / MONITORING AGENCY REPORT NUMBER	
11. SUPPLEMENTARY NOTES			
12a. DISTRIBUTION / AVAILABILITY STATEMENT Distribution authorized to U.S. Government agencies only (proprietary information, Oct 01). Other requests for this document shall be referred to U.S. Army Medical Research and Materiel Command, 504 Scott Street, Fort Detrick, Maryland 21702-5012.			12b. DISTRIBUTION CODE
13. ABSTRACT (Maximum 200 Words) The purpose of this project was to delineate the potential role(s) of excitatory amino acids (EAA) as mediators of central nervous system (CNS) excitation and seizures produced by centrally-active cholinomimetic agents and to evaluate possible palliative treatments for central cholinomimetic toxicity. The scope of this project entails simultaneous use of neurochemical and electrophysiological approaches that are designed to assess cholinomimetic-induced excitation in the rat CNS. The goals for this report period were: (1) to evaluate simultaneously the effects by a direct acting cholinomimetic agent on basal and stimulus-dependent changes in hippocampal EAA levels as well as focal EEG activity, (2) to evaluate simultaneously the effects by an indirect acting cholinomimetic agent on basal and stimulus-dependent changes in hippocampal EAA levels as well as focal EEG activity, and (3) to evaluate the capacity of metabotropic glutamate autoreceptor ligands to attenuate the electrophysiological and neurochemical changes induced by agents referenced in goals (1) and (2). The described studies have been completed and the experimental results support the following general conclusions: (1) elicitation of seizure-like brain wave activity by cholinomimetic agents does not arise principally from a global facilitation of excitatory amino acid mediated neurotransmission within major forebrain pathways; and (2) agents that interact selectively with metabotropic glutamate receptors in the forebrain do not ameliorate substantially the excitatory actions of centrally-active cholinomimetic agents.			
14. SUBJECT TERMS Glutamate, Brain, Cholinomimetics, Seizures, In Vivo Microdialysis, Metabotropic Autoreceptors			15. NUMBER OF PAGES 53
			16. PRICE CODE
17. SECURITY CLASSIFICATION OF REPORT Unclassified	18. SECURITY CLASSIFICATION OF THIS PAGE Unclassified	19. SECURITY CLASSIFICATION OF ABSTRACT Unclassified	20. LIMITATION OF ABSTRACT Unlimited

TABLE OF CONTENTS

<u>SECTION</u>	<u>BEGINNING PAGE</u>
Front Cover	
Report Documentation Page	2
Table Of Contents	3
Introduction	4
Body	4
Key Research Accomplishments	9
Reportable Outcomes	10
Conclusions	10
References	11
Personnel Paid From Contract	11
Appendix I (Figures)	12
Appendix II (Manuscript Preprint)	

INTRODUCTION

The central aim of this project was to investigate and identify any potential role for excitatory amino acids (EAA) as primary or secondary mediators of neuronal excitation and seizures within the central nervous system (CNS) following exposure to centrally-active cholinomimetic agents. While cholinomimetic agents, including the organophosphate (OP) class of acetylcholinesterase inhibitors, cause profound CNS stimulation that is manifest frequently as seizures, convulsions and subsequent neuropathological damage, current strategies designed to protect against or reverse the CNS effects of OP poisoning fail to ameliorate these toxicities. Current evidence implicates glutamate (GLU) and possibly other excitatory amino acids (EAA) in the excitatory and pathophysiological actions of centrally-active cholinomimetics. The overall goals of this project were to critically evaluate the putative role of GLU as a mediator of the central excitatory effects of these agents and to measure directly the ability of metabotropic GLU autoreceptor ligands to protect against and/or reverse the central actions of cholinomimetic agents. The approach to this problem involved simultaneous measurements of electroencephalographic (EEG) activity and intracerebral levels of GLU and L-aspartate (ASP) within the hippocampal formation of rats. The latter measurements were carried out through a novel and highly sensitive technique that facilitates on-line sensitive measurements of extracellular GLU and ASP *in vivo* with an unprecedented degree of temporal resolution. By combining this novel technology with simultaneous electrophysiological measures of cerebral neuronal activity, it was envisioned that any potential role for GLU (or ASP) as mediators of cholinomimetic-induced CNS excitation could be unveiled. Follow-up studies were described wherein the potential utility of metabotropic GLU receptor ligands would be investigated as a possible means to attenuate cholinomimetic-induced changes in central EAA activity and associated excitatory effects on CNS neurons. The information summarized in this final report provides a general review of accomplishments related to the scientific goals of the project during the first two years of the project and specific accomplishments since the previous progress report.

BODY

The major tasks accomplished by this three-year investigation were: (1) the assembly of a new instrument for on-line measurements of GLU and ASP by *in vivo* microdialysis coupled with separation and detection of analytes by capillary electrophoresis and laser-induced fluorescence; (2) characterization of neuronal release of excitatory amino acids from hippocampal neurons during electrical stimulation of the perforant pathway and evaluation of the regulatory influence by metabotropic GLU autoreceptors; (3) an evaluation of the effects by direct and indirect-acting cholinomimetic agents on GLU and ASP levels in the striatum and hippocampus of anesthetized rats; (4) development and validation of an appropriate method to record EEG activity in chloral hydrate-anesthetized rats in a manner that is compatible with simultaneous monitoring of extracellular amino acid transmitters by fast on-line *in vivo* microdialysis; (5) analysis of the temporal and pharmacological relationships between the induction of high-frequency spiking (seizure) activity on EEG recordings and changes in the extracellular concentrations of glutamate (GLU) and aspartate (ASP) following systemic and intracerebral pilocarpine administration; (6) evaluation of the effects by metabotropic autoreceptor ligands on pilocarpine-induced changes in EEG activity and extracellular levels of excitatory amino acids (EAA) in the hippocampal formation; (7)

evaluation of the effects by intracerebral infusion of the organophosphate agent paraoxon on EEG activity and extracellular EAA levels in multiple regions of the hippocampal formation; and (8) effects by metabotropic receptor ligands on paraoxon-induced changes in EEG activity and EAA levels. Detailed summaries of experimental results from the final year of this investigation are provided in the following sections with relevant data depicted in figures and charts located in Appendix I.

Brief Overview of Method to Record EEG Activity and Measure Hippocampal EAA by Fast On-Line Microdialysis in Anesthetized Rats.

The development and validation of a method to measure reliably and simultaneously changes in EEG activity and changes in extracellular EAA levels associated with cholinomimetic drug treatments was crucial for testing the central hypothesis of our original proposal. All recordings of brain electrical activity were conducted with an encephalograph from Grass Medical Instruments (Model 8-10C) with electrodes placed proximal to the dialysis probe in order to obtain focal measures of neuronal electrical activity in the immediate vicinity of the dialysis probe. The recording electrode consisted of a stainless steel wire (150 μ m diameter) that was insulated within a fused silica capillary sleeve (250 μ m, i.d.). Approximately 2mm of wire protruded from the tip of the capillary with insulation removed from the terminal 1mm section. The electrode and microdialysis probe were affixed at a distance of 350 μ m apart with the electrode tip immediately adjacent to the center of the active zone (dialysis membrane) of the microdialysis probe. The microdialysis probe and affixed recording electrode were implanted stereotaxically into hippocampus as described previously. The EEG was derived from the potential between the recording electrode and an isolated ground and reference electrodes located on the scalp and forelimb, respectively. EEG activity was recorded on a desktop personal computer (Gateway, Inc.) through an AT-MIO-16 data acquisition board at 100-500Hz band frequency. Fourier transforms of electroencephalograms were carried out with software (TS-find) obtained from Dr. R. Mark Wightman at the University of North Carolina (Chapel Hill, NC). Initial recordings of global EEG activity were used to isolate and identify and eliminate artifactual interferences (noise) from other instruments and unrelated sources. In anesthetized rats, EEG recordings exhibited normal properties, including low amplitude spiking with less frequent occurrences of high-frequency spike complexes.

Pharmacological Regulation of Pilocarpine-Induced Reductions in Hippocampal Basal and Stimulated EAA Levels: Reversal Following Metabotropic Receptor Activation.

In the original proposal, we had hypothesized that direct-acting or indirect-acting cholinomimetic agents would mimic the CNS actions of centrally-active organophosphate (OP) agents. Previously, we had reported successful induction of seizure-like changes in EEG activity of anesthetized rats following intracerebral infusion of pilocarpine (10mM) into various regions of the hippocampal formation. However, in spite of that success, an unexpected outcome from those preliminary studies was the observation that pilocarpine caused a rapid and sustained decrease in the basal extracellular levels of GLU and ASP in the hippocampus. Additional studies during the final year have provided confirmatory results and demonstrated unequivocally that pilocarpine infusion reduces rather than elevates resting (basal) EAA levels in the hippocampal formation. In order to confirm that neurons in the immediate vicinity of the delivery site for pilocarpine (i.e., the dialysis probe) were exhibiting

high frequency high amplitude spike activity, recording electrodes were placed at various locations within the hippocampus, including dentate gyrus, CA1 and CA3 regions. A schematic representation of loci for placement of the dialysis probe and recording electrodes is shown in the top portion of FIGURE 1. Probe and electrode placements were confirmed histologically in postmortem slices. As shown in FIGURE 1 (panel B), infusion of pilocarpine by reverse dialysis caused an immediate appearance of seizure-like waveforms in the EEG as recorded by electrodes placed proximal to the dialysis probe. At later times, the epileptiform activity patterns became constant and spread generally into all recording sites. However, as reported previously, extracellular GLU levels decreased gradually with a markedly slower time course and never exhibited any evidence for an increasing in basal levels as proposed in our original proposal. This result was unexpected and contradicts our original hypothesis insofar as drug-induced seizure activity was expected to be accompanied by a marked elevation in EAA levels. However, since basal (non-stimulated) levels of GLU and ASP in hippocampus and striatum are known to be poorly regulated and dissociated from neuronal firing activity, as revealed by the absence of calcium-dependence and tetrodotoxin sensitivity (see summarized data in FIGURE 2), we speculated that basal EAA levels may provide an incomplete measure of pilocarpine action. Therefore, a series of studies were carried out in which electrical stimulation of the perforant pathway was performed in order to fully activate glutamatergic fibers that project throughout the hippocampal formation. By using this approach, it is possible to evaluate directly the impact by pilocarpine infusion on the release of GLU from hippocampal neurons and thereby feasible to gain better insight into the effect of this cholinomimetic agent on GLU-mediated synaptic transmission. As shown in FIGURE 3, brief perforant path stimulation by means of a 20 s train of square-wave depolarizing pulses elicits an instantaneous rise (within the limits of our temporal resolution) in the extracellular GLU level. The response of GLU to successive stimulations was highly reproducible with no significant changes in the maximal peak height, total duration, or peak area across four successive stimulus trains when applied at 30-min intervals. In contrast to these results for GLU, extracellular levels of ASP exhibited small and highly variable changes following perforant stimulation and, therefore, data were not analyzed for stimulus-dependent changes.

Using this paradigm for direct activation of glutamatergic neurons, we evaluated the net evoked release of GLU at various times following intrahippocampal pilocarpine infusion. As shown in FIGURE 4, pilocarpine treatment caused a complete and prolonged suppression of the rise in hippocampal GLU levels associated with perforant path stimulation. The attenuation of stimulated GLU responses was rapid with a complete ablation occurring within the initial five minute period of pilocarpine infusion. While this observation parallels the overall decline in basal GLU levels, the effect on stimulus-dependent GLU release appeared to transpire more quickly and to a much greater extent. Nevertheless, in light of the uncharacterized contribution by neuronally derived (synaptic) GLU release to the total extracellular pool of GLU in the hippocampal formation, it remains possible that pilocarpine induced suppression of basal GLU levels is a reflection of the apparent uncoupling of neuronal GLU release from stimulated neuronal firing activity. While our results do not provide proof for this proposed uncoupling between depolarization and GLU release, the data summarized in FIGURE 4 provide compelling evidence for such an action insofar as direct application of a supramaximal depolarizing stimulus to the perforant pathway fails to elicit any measurable GLU synaptic overflow.

Despite the unexpected yet consistent inhibitory effect by pilocarpine on hippocampal GLU levels, we decided to carry out preliminary assessments of potential interactions between metabotropic GLU receptor ligands and pilocarpine as outlined in the original proposal. Although the effects by pilocarpine on basal and stimulated levels of GLU were inconsistent with our original hypothesis, this line of investigation was followed briefly in view of the atypical effects produced by metabotropic receptor ligands in the hippocampal formation relative to other brain regions. As noted briefly in a previous report, metabotropic autoreceptors on hippocampal neurons exhibit marked differences from receptors on corticostriatal neurons. As summarized in FIGURE 5, local intra-hippocampal infusion of the metabotropic GLU receptor agonist ACPD fails to alter GLU overflow in hippocampus following perforant path stimulation, whereas infusion of the antagonist MCPG causes a significant elevation in stimulated GLU overflow. These results differ substantially from data obtained in striatum where these drugs evoke actions that are more typical of a presynaptic autoinhibitory process (FIGURE 5). Local infusion of the GLU transport inhibitor PDC points out an additional difference between regulatory controls for hippocampal and striatal glutamatergic neurons and underscore a substantially greater role for GLU transport within hippocampal pathways.

Despite the somewhat atypical regulatory role of metabotropic autoreceptors in hippocampus, we decided to carry out a preliminary test of the interaction between ACPD and pilocarpine in our anesthetized rat model. These studies were proposed within our original proposal and represented a key component of the project. However, in view of the seemingly contradictory results outlined above, studies were carried out on a limited basis. Data from these experiments are summarized in FIGURES 6 and 7. Initial studies were carried out with the metabotropic receptor agonist ACPD and were designed to determine whether pilocarpine-induced decreases in hippocampal basal GLU levels would be influenced by this metabotropic receptor agonist. As shown in FIGURE 6, infusion of ACPD (200 μ M) caused an unexpected rise in GLU levels in rats that had been subjected to a prior infusion of pilocarpine. The effect by ACPD, which was notably rapid in its onset (FIGURE 6), was not expected to occur in view of the modest inhibitory effect by this agent when administered alone (FIGURE 2). Despite the unexpected nature of this experimental observation, the result was consistent in four animals that were tested and was deemed to be highly reproducible. However, similar results were not obtained for stimulus-evoked responses following perforant path stimulation. As shown in FIGURE 7, pilocarpine treatment suppressed the evoked rise in GLU levels associated with perforant path stimulation. However, local infusion of ACPD failed to restore the normal GLU response to perforant path stimulation in these animals. In light of these results, it appears that the metabotropic receptor agonist ACPD acts to oppose the suppression of basal GLU levels produced by local pilocarpine infusion but fails to influence the suppression of evoked GLU overflow associated with perforant path stimulation.

Additional studies were performed but, in general, have failed to clarify the mechanistic nature of the effect by ACPD. Limited studies (two rats) revealed that the ability of ACPD to reverse pilocarpine-induced suppression of basal GLU levels was not reversible by the metabotropic receptor antagonist MCPG (FIGURE 6). Infusion of MCPG at the same time or 15 min prior to infusion of ACPD had no effect on the response to ACPD. Since MCPG is an effective and potent antagonist at all subtypes of metabotropic GLU receptors, this result strongly indicates that ACPD-induced elevation of extracellular GLU levels may involve a mechanism that is distinct from metabotropic receptor activation. While the limited

results obtained here support such a conclusion, speculation regarding possible alternative explanations for the actions by ACPD would be unwarranted at this time. However, a related observation led to diminished interest in this line of investigation. As noted above, pilocarpine infusion produces a reliable appearance of high frequency high amplitude waveforms in EEG activity that is indicative of seizureogenic effects by this drug. Previous results (see year 2 Progress Report) revealed a clear dissociation between the seizure-promoting effects of pilocarpine and a hypothesized facilitation of GLU-mediated transmission in the hippocampus. Nevertheless, in view of the intriguing interactions between ACPD and pilocarpine with respect to extracellular GLU levels in hippocampus, it seemed reasonable to determine whether ACPD treatment exerted any influence on EEG changes associated with pilocarpine treatment. As expected, ACPD failed to produce any notable change in the seizure-promoting actions of pilocarpine (data not shown). The absence of any appreciable effect by ACPD on EEG activity provided further evidence of a disassociation between EEG activity and basal or stimulated levels of GLU within the hippocampus. In view of these results, studies related to this line of investigation were discontinued.

Intracerebral Infusion of an Organophosphate Compound.

In order to confirm that results with pilocarpine and physostigmine (see previous reports) were representative of the actions produced by the organophosphate class of indirect-acting cholinomimetic agents, representative studies were repeated with *O,O*-diethyl *O*-(4-nitrophenyl)-phosphate or paraoxon. In view of our successful use of pilocarpine when administered via an intracerebral route, a similar approach was used for paraoxon. A major advantage of this paradigm was the ability to avoid the substantial peripheral toxicity associated with systemic drug treatments and to diminish the loss of subjects due to uncontrollable systemic actions. By direct application of paraoxon into the hippocampal formation via reverse dialysis, it was possible to isolate and study the direct central actions of this highly toxic agent.

The effects of paraoxon were investigated under conditions identical to those described previously for studies with pilocarpine and physostigmine in order to minimize any possible differences associated with the experimental model. In order to determine that an appropriate treatment regimen for paraoxon was used, preliminary studies were performed using EEG recordings as an index of the onset of drug action. Following application of different paraoxon concentrations for periods of 5 to 45 min, it was determined that a 20 min infusion of 50 μ M paraoxon resulted in the appearance of high frequency high amplitude spikes on the EEG recording (FIGURE 8). In view of this, all subsequent studies were conducted using this drug treatment regimen. The goal of these experiments was to ascertain whether paraoxon, an irreversible organophosphate class inhibitor of acetylcholinesterase, would produce a spectrum of changes that paralleled the effects on extracellular GLU levels in hippocampus described previously for pilocarpine and physostigmine. Following paraoxon infusion into the hippocampus via reverse dialysis, GLU levels exhibited no significant change from the pre-drug baseline level. As shown in FIGURE 9A, basal GLU levels in the hippocampus drifted down slightly during a 2.5 hour period following drug infusion. However, despite the absence of any remarkable changes in extracellular GLU levels, high frequency high amplitude spiking activity on EEG records (FIGURE 8) provided evidence for paraoxon-induced seizure activity in neurons proximal to the dialysis probe. In a separate group of animals, EAA transport was inhibited via local infusion of PDC prior to paraoxon

treatment. The rationale for this investigation was based upon our previous determination that GLU transport is an extremely important factor for controlling synaptic GLU overflow in the hippocampus (see above). In view of the highly efficient removal of GLU by active transport, it seemed plausible that any enhanced release of GLU following paraoxon infusion could be buffered completely by the action of EAA transporters located within or adjacent to glutamatergic synapses. Direct experimental testing of this hypothesis provided data that appeared to support this idea. As shown in FIGURE 9B, pretreatment with PDC caused a greater than five-fold elevation in basal GLU levels. Under these conditions of attenuated GLU transport, infusion of paraoxon caused a small but consistent increase in extracellular GLU. Close inspection of these data indicate that extracellular GLU levels began to rise during the 20 min infusion period for paraoxon and appeared to remain elevated throughout the remainder of the 2.5 hour sampling period. In view of these results, it appears that paraoxon exposure may actually elevate GLU levels within the hippocampal formation of anesthetized rats. Although the effect appears to be relatively modest, it must be noted that extracellular GLU derives from multiple sources. In light of this, it is possible that paraoxon induces a marked rise in synaptic GLU levels which are manifest as the relatively modest increase observed here.

KEY RESEARCH ACCOMPLISHMENTS

- demonstration that pilocarpine-induced reduction in basal (non-stimulated) hippocampal EAA levels can be attenuated through metabotropic glutamate receptor activation.
- demonstration that the seizureogenic effects of pilocarpine (intracerebral) are accompanied by a complete inhibition of perforant path stimulated GLU overflow in the hippocampus
- demonstration that the seizureogenic effects of pilocarpine are not influenced significantly by metabotropic glutamate receptor ligands. This results contradicts one of the major expected outcomes for this project.
- demonstration that intracerebral delivery of the organophosphate agent paraoxon produces a delayed appearance of high frequency waveform activity in the EEG of chloral hydrate-anesthetized rats. These results indicate successful induction of limbic seizure activity in our anesthetized animal model.
- demonstration that paraoxon causes a rapid but modest rise in extracellular GLU in the hippocampal formation under conditions of attenuated EAA transport.

D. REPORTABLE OUTCOMES

Reportable outcomes for this project include the following items. Arrow indicates item included in appendix of this report. Manuscripts that are submitted but not yet accepted for publication have not been included. All other items have been submitted previously.

- Kennedy, R.T., Witowski, S., Thompson, J. and Boyd, B. (1999) Capillary electrophoresis and capillary chromatography for *in vivo* monitoring of amino acid and peptide neurotransmitters. *Proceedings Of The 8th International Conference On In Vivo Methods: Monitoring Molecules In Neuroscience*. June 19-23.
- Witowski, SR and Kennedy, RT (1999). Monitoring neurotransmitter amino acids by microdialysis with on-line flow gated capillary electrophoresis. *Proceedings Of The 8th International Conference On In Vivo Methods: Monitoring Molecules In Neuroscience*. June 19-23.
- Kennedy, RT, Vickroy, TW, Witowski, SR, Thompson, JE, Boyd, B and Phillips, I (1999). Monitoring amino acid neurotransmitters in vivo with high temporal resolution using microdialysis. *Neuroscience Abstr.* **25**: 2232.
- Kennedy, RT, Vickroy, T, Witowski, SR, Thompson, JE and Boyd, B (1999). Monitoring Amino Acid Neurotransmitters In Vivo With High Temporal Resolution Using Microdialysis, Society for Neuroscience Abstracts.
- Witowski, SR (2000). Monitoring Neurotransmitter Amino Acids in Vivo by Microdialysis With On-Line Flow-Gated Capillary Electrophoresis, doctoral dissertation, University of Florida.
- ➔ • Kennedy, RT, Thompson, JE and Vickroy, TW (2001). In vivo monitoring of amino acids by direct sampling of brain extracellular fluid at ultralow flow rates and capillary electrophoresis, *J. Neurosci. Meth.* (in press).
- Witowski, SR, Vickroy, TW and Kennedy, RT. Regulation of Synaptic Glutamate Overflow in Hippocampus Following Perforant Path Stimulation In Vivo: Evidence for Volume Transmission. (submitted to *Brain Research*).
- Bowser, MT and Kennedy, RT. High Resolution Monitoring of Amines In Vivo by CE-LIF. (submitted to *The Analyst*).

E. CONCLUSIONS

The results of work conducted during the final year of this investigation are consistent in several ways with results reported in previous annual reports and, in general, tend to support and strengthen the preliminary conclusions that were drawn last year. Results obtained with three different cholinomimetic agents, namely the direct-acting muscarinic

agonist pilocarpine and the indirect acting agents physostigmine and paraoxon, support the conclusion that the seizureogenic action of cholinomimetic agents does not arise directly from enhanced neuronal excitability associated with enhanced glutamatergic transmission. This conclusion represents a rejection of the central hypothesis upon which this project was based and appears to discount any possible use of drugs that act upon the metabotropic class of GLU receptors as potential preventative or symptomatic treatments for CNS stimulation associated with cholinomimetic exposure. In light of these experimental findings, we do not foresee any reasonable justification for future studies related to this line of investigation.

F. REFERENCES

Chapman, A. G. *Glutamate receptors in epilepsy in Prog. Brain Res. v 116*. Ottersen, O. P.; Langmoen, I. A.; Gjerstad, L., eds. Elsevier, NY 1998, 371.

Kullman, D. M.; Asztely, F. *Trends Neurosci.* 1998, 21, 8.

Kullman, D. M.; Erdemli, G.; Asztely, F. *Neuron*, 1996, 17, 461.

McDonough, J. H.; Shih, T. M. *Neurosci. Biobehav. Rev.* 1997, 21, 559.

Saugstad, J. A.; Kinzio, J. M.; Mulvihill, E. R.; Segerson, T. P.; Westbrook, G. L. *Mol. Pharmac.* 1994, 45, 367.

Smolders, I.; Khan, G. M.; Lindekens, H.; Prikken, S.; Marvin, C. A.; Manil, J.; Ebinger, G.; Michotte, Y. *J. Pharm. Exp. Ther.* 1997, 283, 1239.

Smolders, I.; Khan, G. M.; Manil, J.; Ebinger, G.; Michotte, Y. *Brit. J. Pharmacol.* 1997, 121, 1171.

Smolders, I.; Van Belle, K.; Ebinger, G.; Michotte, Y. *Eur. J. Pharmacol.* 1997, 319, 21.

G. PERSONNEL PAID FROM CONTRACT

T.W. Vickroy
R.T. Kennedy

S.R. Witowski
M.E. Bowser

H. APPENDICES

Appendix I: The figures on the following pages are related to experimental results that are summarized above in the BODY of this report (Section B). The figures are arranged in the same order in which they are discussed in Section B.

Appendix II: copy of manuscript in press

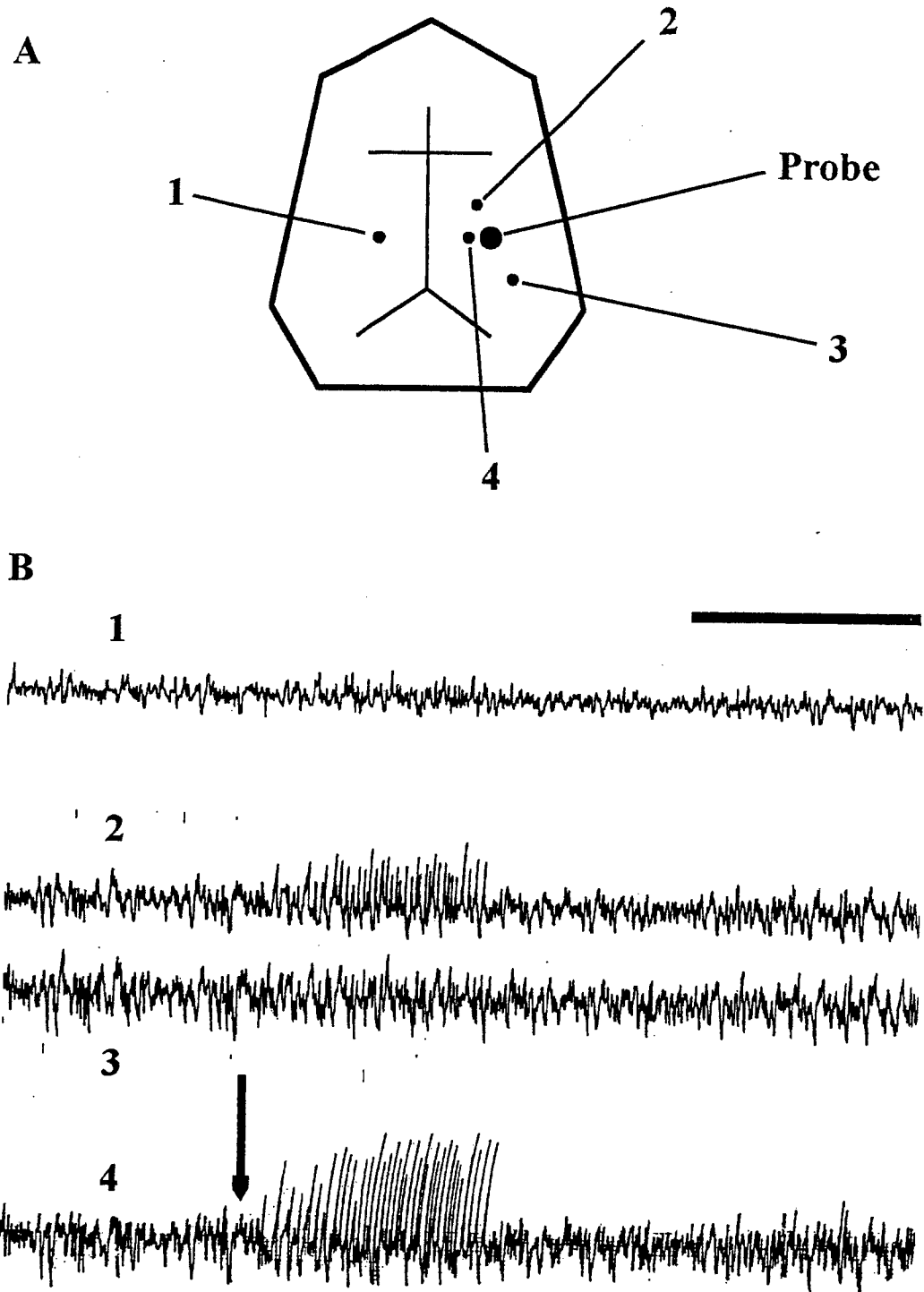


FIGURE 1. Effect of Intrahippocampal Pilocarpine (10mM) Infusion on Focal EEG Activity in Anesthetized Rats. Recording electrodes (numbers 1 through 4 in Figure A) were placed stereotaxically at selected sites proximal or distal to the microdialysis probe. Recordings were made in the dentate gyrus in the opposite hemisphere (1), two locations within the CA1/CA3 lamina (2 and 3) and the dentate gyrus/CA1 region (4). **PANEL B:** EEG tracings from the four electrodes are depicted before and after the start of pilocarpine infusion (arrow). Bar width represents 10 sec.

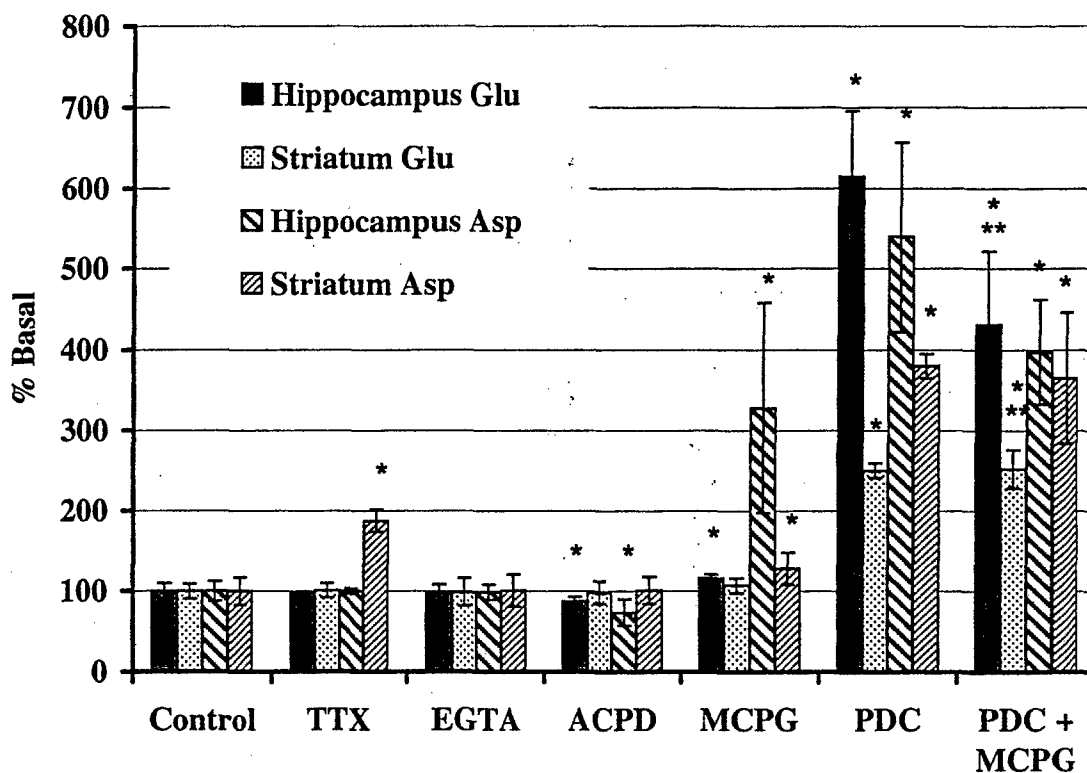


FIGURE 2. Regulation of Basal Levels of Glutamate and Aspartate in Hippocampus and Striatum of Anesthetized Rats. Basal levels of GLU and ASP were 310 ± 40 and 87 ± 11 nM, respectively. All values are expressed as percent (mean \pm S.E.M., n=4) of drug-free control values in each experimental subject. Drugs were infused via reverse microdialysis for 30 min prior to measurements.

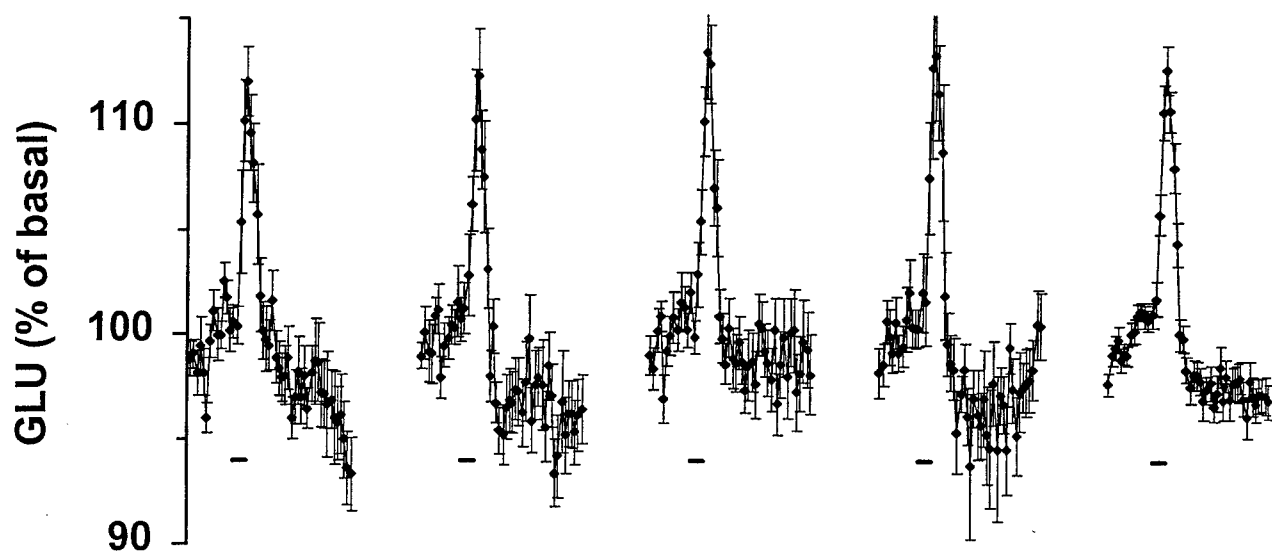


FIGURE 3. Evoked Release of Glutamate in Hippocampus Following Perforant Path Stimulation. Each point represents the level for the compound indicated obtained from a given electropherogram. Each point is the mean \pm SEM from 20 rats. Levels reported relative to the basal level determined from the average of 10 consecutive electropherograms taken just prior to the beginning of the traces shown. Bar indicates application of 20 Hz stimulation and corresponds to 20 s. Position of bar is corrected for dead volume of system. From left to right, each trace represents averaged data from four successive stimulation trains at 30-min intervals in all rats. The far right trace is the average (ave) of all stimulations.

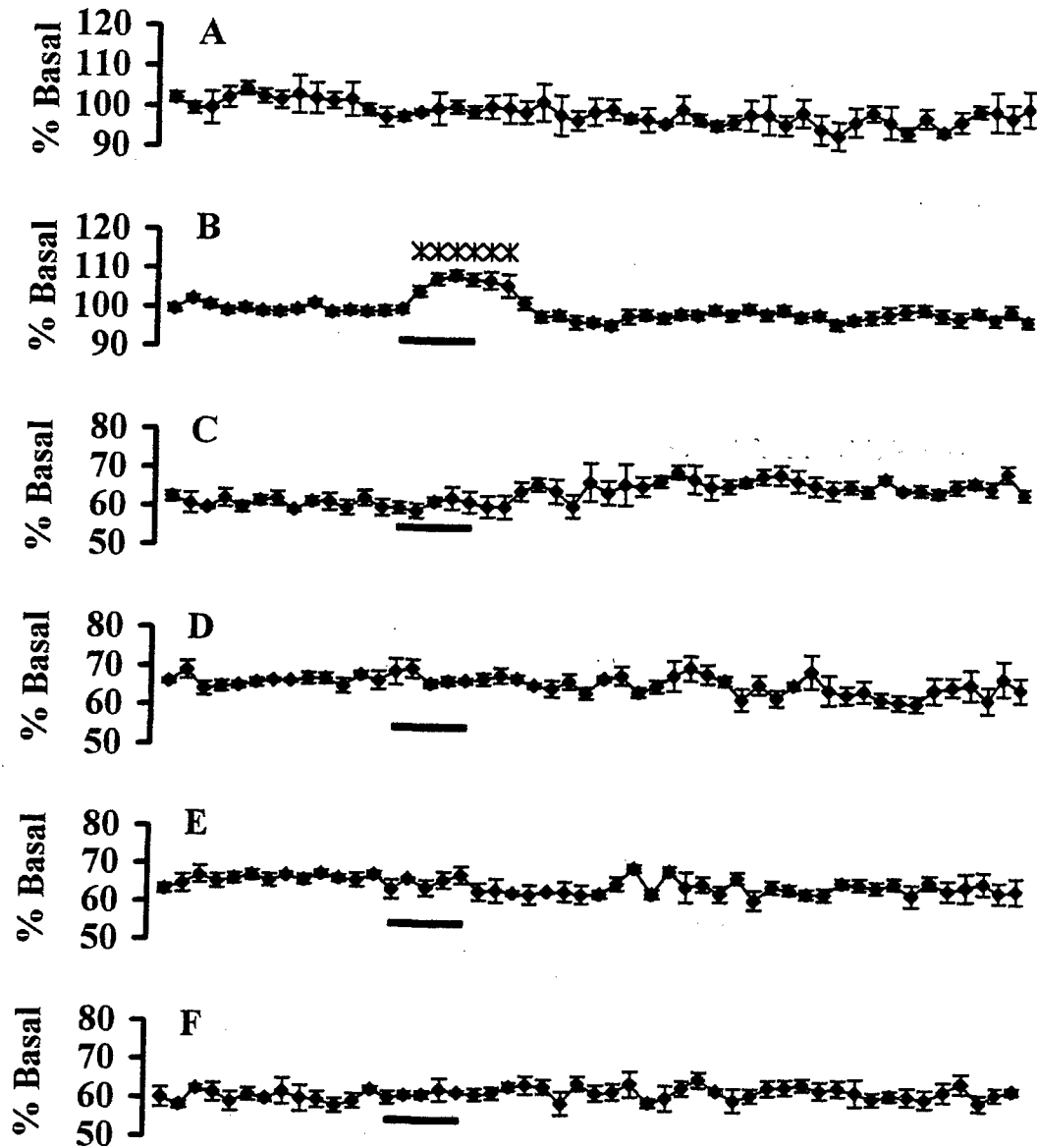


FIGURE 4. Effect by Pilocarpine Infusion on Evoked Glutamate Release in Hippocampus Following Perforant Path Stimulation. Data points represent the mean \pm SEM of glutamate levels ($n=16$ stimulations in 4 rats) expressed as a percent of basal levels in each animal. Trace A represents basal levels in unstimulated control subjects. Horizontal bar corresponds to the application of a 20 sec stimulus of the perforant path. Trace B depicts control responses in all subjects immediately before the infusion of pilocarpine (10mM). Traces C through F represent basal and stimulated glutamate levels after 19 min (C), 39 min (D), 59 (E) and 80 min (F) following pilocarpine infusion. Asterisks indicate a significant increase in glutamate levels relative to pre-stimulus basal levels.

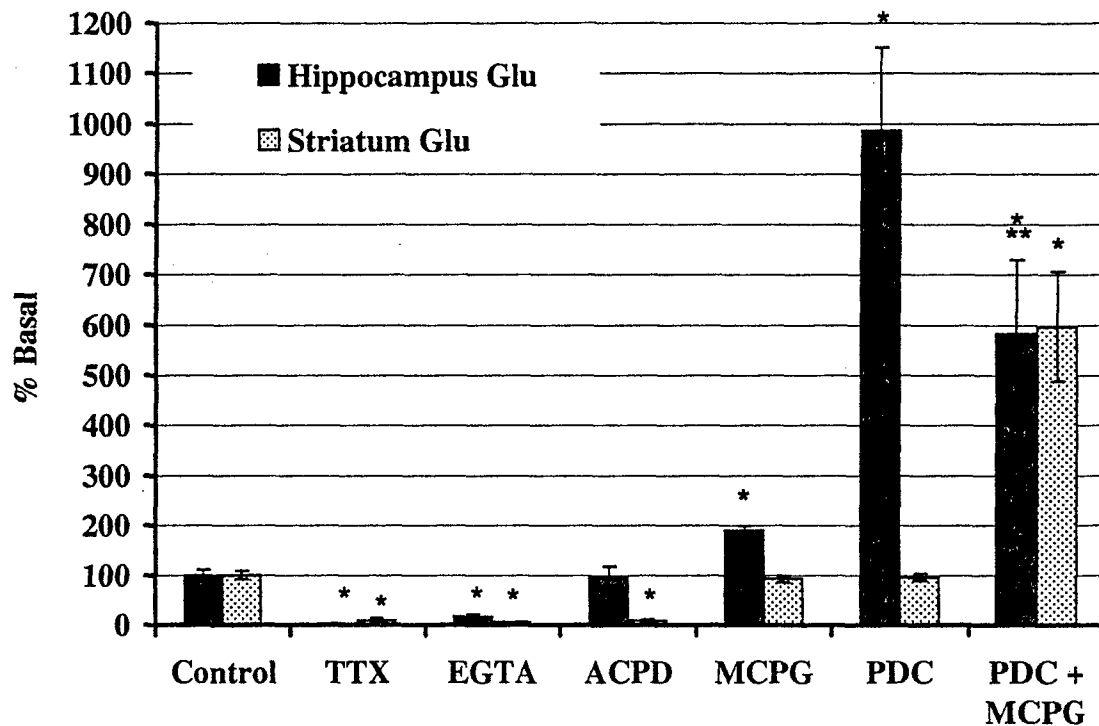


FIGURE 5. Regulation of Stimulated Levels of Glutamate in Hippocampus and Striatum of Anesthetized Rats. Evoked responses in hippocampus and striatum were 66.5 ± 7.3 fmol ($n=80$ stimulations, 21 rats) and 380 ± 48 fmol, respectively. All values are expressed as percent (mean \pm S.E.M., $n=16$, 4 rats) of drug-free control values in each experimental subject. Drugs were infused via reverse microdialysis for 30 min prior to measurements.

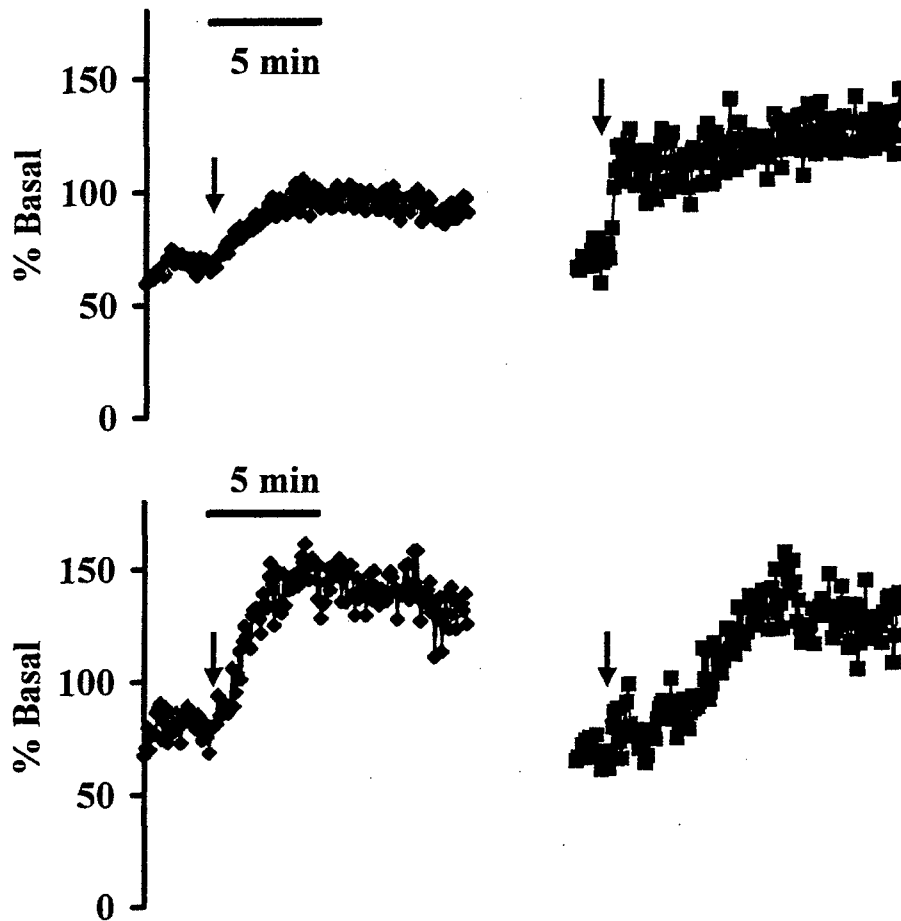


FIGURE 6. Effect by ACPD in Pilocarpine-Treated Rats. Individual tracings are from 4 separate rats that had been pretreated with pilocarpine (10mM via intrahippocampal infusion) for 15 to 30 min. Arrows indicate the initiation of ACPD (200 μ M) infusion.

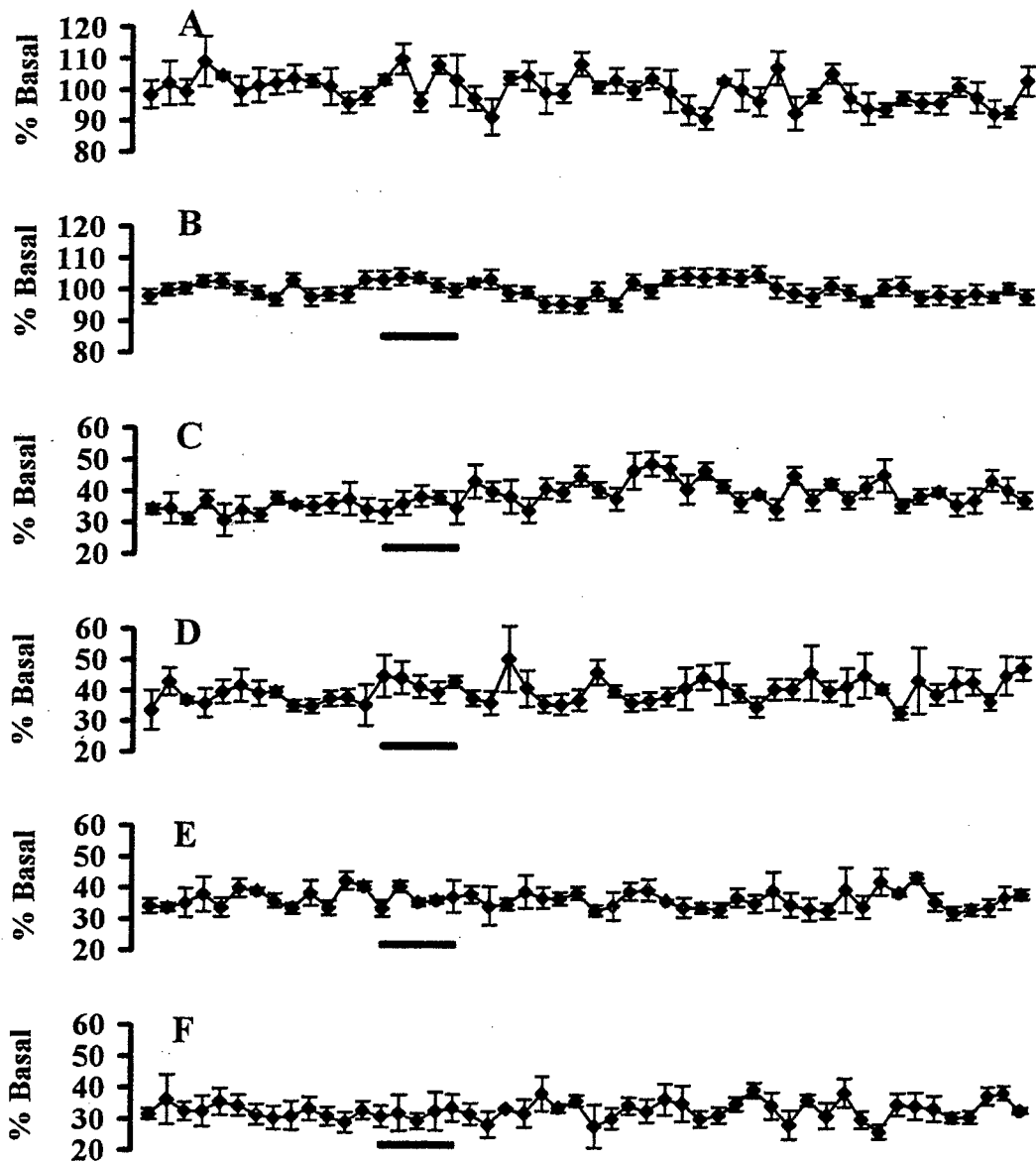


FIGURE 7. ACPD Infusion Fails to Reverse Pilocarpine-Induced Suppression of Stimulus-Dependent Glutamate Release in Hippocampus. Experimental protocol is similar to that described for FIGURE 4. Trace A represents a control (non-stimulated) tracing, whereas traces B through F represent tracings from pilocarpine-treated rats at 0, 5, 10, 20 and 45 min following ACPD infusion.

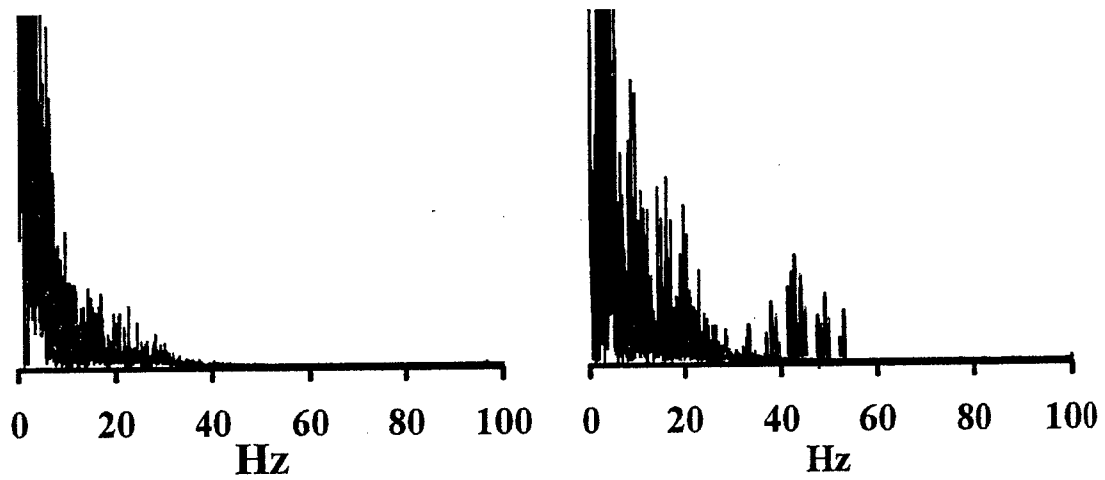


FIGURE 8. Induction of Seizure-Like EEG Activity by Intracerebral Infusion of Paraoxon. Plots represent averaged Fourier transforms of EEG recordings from 3 rats before (left) and 30 min following the infusion of paraoxon ($50\mu\text{M}$, 20 min).

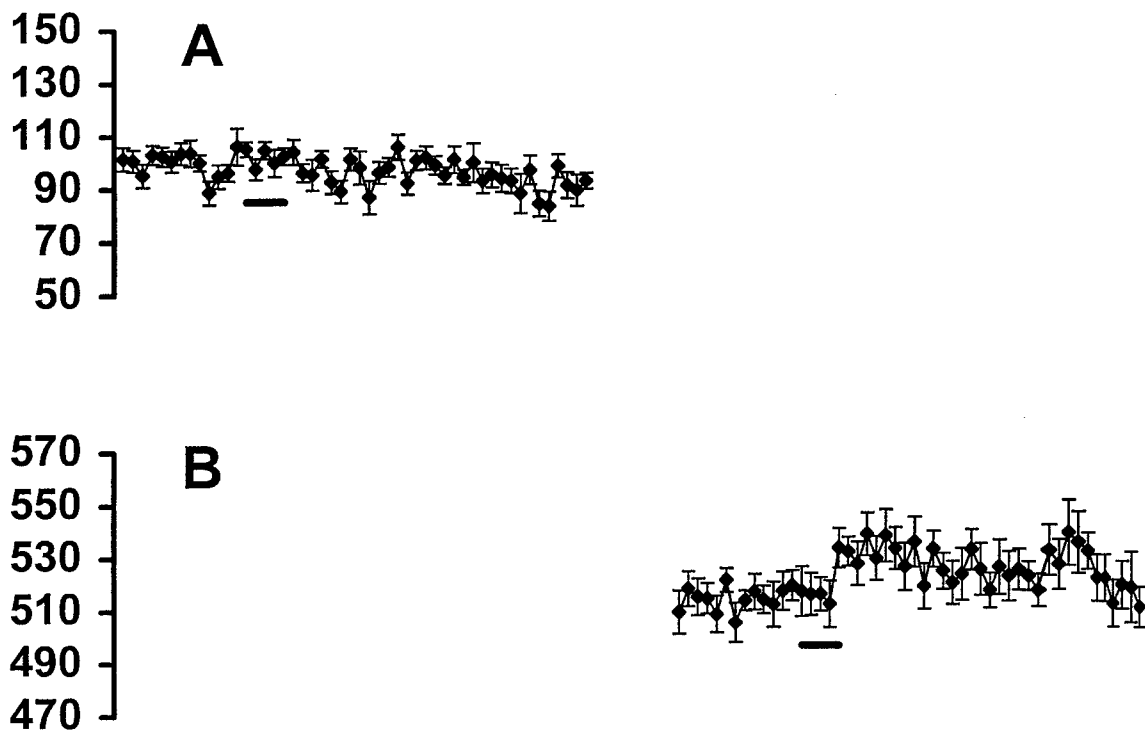


FIGURE 9. Effect of Paraoxon Treatment on Basal Glutamate Levels in Rat Hippocampus. Panel A depicts glutamate levels (percentage of pre-drug level expressed as mean \pm SEM, n=4 rats) in response to paraoxon infusion (solid bar). Panel B depicts glutamate levels in rats pretreated with the EAA transport inhibitor PDC as described in text. Bar indicates timing of paraoxon treatment. Individual measurements of glutamate levels were performed at 5 min intervals.

original
file

**In Vivo Monitoring of Amino Acids by Direct Sampling of Brain Extracellular Fluid at
Ultralow Flow Rates and Capillary Electrophoresis**

Robert T. Kennedy^{1*}, Jonathan E. Thompson¹, and Thomas W. Vickroy²

¹ Department of Chemistry, P.O. Box 117200, University of Florida, Gainesville, FL 32611-7200

² Department of Physiological Sciences, University of Florida, Gainesville, FL 32611

* To whom correspondence should be addressed

Corresponding Author Contact:

Phone: (352)392-9839

Fax: (352)392-4582

Email: rtkenn@chem.ufl.edu

Keywords: microdialysis, excitatory amino acids, glutamate, GABA, direct sampling, in vivo monitoring, laser-induced fluorescence

Abstract

Extracellular levels of glutamate (GLU), aspartate (ASP), glycine (GLY), phosphoethanolamine (PEA), and γ -aminobutyric acid (GABA) were measured in the striatum of anesthetized rats using a novel sampling approach in which extracellular fluid was removed at 1-50 nL/min using a fused silica capillary tube with 18 to 40 μm inner diameter and a outer diameter of 90 μm . The samples of extracellular fluid were analyzed by capillary electrophoresis with laser-induced fluorescence detection. Basal levels for GABA, GLY, and GLU measured using direct sampling at 1 nL/min were 270 ± 40 , 4950 ± 1100 , and 1760 ± 150 nM respectively in good agreement with values obtained using microdialysis sampling calibrated by the low-flow rate method. ASP levels were approximately 4-fold higher in directly sampled fluid than in dialysate. At higher direct sampling flow rates (10 to 50 nL/min), detected levels of the amino acids were lower by 70 to 90% indicating depletion of analyte under these conditions. PEA, an indicator of membrane disruption, was 5.5-fold higher in dialysate than in directly sampled extracellular fluid indicating greater tissue damage associated with microdialysis. In addition to the basal measurements, the direct sampling technique was applied to monitoring concentration changes of GLU and ASP in the striatum with better than 90 s temporal resolution after perfusion of either 120 mM K^+ or 400 μM L-trans-pyrrolidine-2,4-dicarboxylic acid (PDC) through a microdialysis probe immediately adjacent to the direct sampling capillary. Levels of glutamate and aspartate increased 615 ± 95 and 542 ± 96 % respectively ($n = 4$) upon addition of 120 mM K^+ to the perfusate and 622 ± 234 and 672 ± 218 % ($n = 5$) for PDC. It is concluded that direct sampling at low flow rates allows determination of extracellular levels of the amino acids with spatial resolution that is at least 500-fold better than microdialysis.

Introduction

The extracellular compartment of the brain is a complex, dynamic microenvironment containing chemical signals, metabolites, and nutrients. Chemical analysis of this environment *in vivo* has led to important insights into neuronal and glia communication and function. The interest in *in vivo* monitoring of the extracellular fluid has been heightened by the discovery of volume transmission in which neurotransmitters escape the confines of the synaptic cleft and activate other receptors in the vicinity of the release site (Zoli et al., 1998).

Both sensor and sampling approaches have been employed to monitor neurotransmitters and related compounds in the extracellular fluid of the brain. Sensors are advantageous in that they can provide high spatial and temporal resolution (Kawagoe et al., 1992; Kulagina et al., 1999; Burmeister and Gerhardt, 2001; Georganopoulou, 2001). In the best case, sensors have response times ≤ 0.1 s with spatial resolution of a few micrometers. Sensors with these capabilities are available for only a few analytes and are usually restricted to monitoring one analyte at a time. An alternate strategy involves collecting samples from the extracellular fluid and analyzing fractions either off-line (Ungerstedt and Hallstrom, 1987) or on-line (Chen and Lunte, 1995; Zhou et al., 1995; Lada et al., 1997).

One approach to *in vivo* sampling is push-pull perfusion in which two concentric tubes with a total diameter of 500 μm are implanted in or near the brain region of interest. Sampling is accomplished by flowing in one tube and out the other tube at a flow rate of ~ 10 $\mu\text{L}/\text{min}$ (Gaddum, 1961; Izquierdo and Izquierdo, 1971; Myers, 1972). This method has fallen out of favor, except for neuropeptide monitoring, because of the large perturbation of the tissue caused by perfusion of the tissue. Push-pull perfusion has been largely supplanted by microdialysis sampling (Ungerstedt and Hallstrom, 1987; Ungerstedt 1991). In microdialysis, molecules in the

extracellular fluid diffuse across a semi-permeable membrane into a flowing stream of solution which is collected for analysis. Microdialysis has emerged as the most important method for in vivo sampling because tissue perturbation is considerably reduced since the tissue is not directly bathed with a perfusate. Despite the popularity of the technique, microdialysis is not without shortcomings. Microdialysis has poor spatial resolution because the probes are usually 1-4 mm long and 200 μm diameter. Therefore, it is of limited use for small brain nuclei or heterogeneous brain regions. In addition, temporal resolution can be poor because sufficient sample must be collected for analysis. Typical sampling times are 5-15 min (Kissinger, 1991; Herrera-Marschitz et al., 1996); however, the recent implementation of sensitive analytical methods coupled to microdialysis has pushed the temporal resolution to a few seconds (Tucci et al., 1997; Robert et al. 1998; Lada et al., 1998; Boyd et al., 2000). Finally, obtaining quantitative estimates of extracellular concentrations by microdialysis is problematic because the relative recovery obtained by in vitro experiments does not match that obtained in vivo (Marsden et al., 1986; Lerma et al., 1986; Benveniste, 1989). In vivo calibration methods (Justice, 1993) such as the no-net flux (Lonnroth et al., 1987; Parsons et al. 1991) and low-flow rate method (Wages et al., 1987) are available, but problems persist in their use (Peters and Michael, 1998; Bungay et al., 2001).

In an attempt to improve spatial resolution and quantification for in vivo monitoring we have explored direct sampling of brain extracellular fluid using miniaturized probes that are 60-90 μm diameter and remove fluids at 1-50 nL/min without the use of a "push" fluid. In this work, we have examined the feasibility of using this sampling approach to determine the extracellular levels of neuroactive amino acids. We have investigated: 1) the effect of sampling

flow rate on the measurement, 2) the possibility of monitoring changes in transmitter levels in vivo, and 3) the spatial and temporal resolution of direct sampling.

Methods

Reagents and Materials. Amino acids, derivatization reagents, KCl, L-trans- pyrrolidine-2,4-dicarboxylic acid and chloral hydrate were from Sigma (St. Louis, MO) and were used as received. MgSO₄, CaCl₂, NaCl, NaOH and boric acid were from Fisher Scientific (Pittsburgh, PA). Hydroxypropyl β-Cyclodextrin was from Aldrich Chemical Company (Milwaukee, WI). Artificial cerebral spinal fluid (aCSF) consisted of 145 mM NaCl, 2.68 mM KCl, 1.01 mM MgSO₄, and 1.22 mM CaCl₂. High K⁺ CSF consisted of 27 mM NaCl, 120 mM KCl, 1.01 mM MgSO₄, and 1.22 mM CaCl₂. All solutions were prepared from purified, deionized water from a Millipore Milli-Q water purification system (Milford, MA). All fused silica capillaries were from Polymicro Technologies (Phoenix, AZ).

Animal and Surgical Procedures. All experimental uses of laboratory rats were reviewed and approved by the University of Florida Institutional Animal Care and Use Committee and conform with policies and procedures set forth by U.S. Public Health Service Policy on Humane Care and Use of Laboratory Animals. Male Sprague-Dawley rats weighing 250-350 g were allowed free access to food and water. The animals were anesthetized with subcutaneous injections of 100 mg/mL chloral hydrate at a dose of 400 mg/kg animal weight. Additional injections of 200 mg/kg were performed every 30 minutes until the animal no longer exhibited limb reflex. The animal was then secured in a stereotaxic apparatus (David Kopf Instruments, Tujunga, Ca.) and the probe inserted into the striatum at a rate of approximately 20 μm/s. Coordinates used for this analysis were +0.02 AP, -0.30 ML, -0.65 cm DV from bregma. A

recovery time of 1 hour was allowed after insertion of the sampling probe prior to collection of samples to allow stabilization of neurotransmitter basal levels.

Sampling. The direct sampling probe consisted of 1 to 3 meters of 18 μm inner diameter (I.D.) by 90 μm outer diameter (O.D.) fused silica capillary for sampling at 1-10 nL/min. For sampling at 50 nL/min the capillary was a 2 m length of 40 μm I.D. by 90 μm O.D. tubing. To provide greater rigidity for the probe, the sampling end of the capillary was threaded through a 150 μm I.D. by 360 μm O.D. capillary such that 1 mm of the sampling capillary was exposed and then glued in place with cyanoacrylate cement. Prior to implantation, the direct sampling capillary was filled with aCSF. After implantation, a 90 min recovery period was allowed before sampling commenced. Sampling times lasted 90 to 270 min. To generate sampling flow, vacuum was applied to the outlet end of the sampling capillary by a vacuum pump. Outlet pressures of 100-500 mm Hg were used to generate the desired flow rate. In initial experiments, sampling flow rates were measured both before and after an in vivo experiment through the use of a UV-vis absorbance detector placed on-line with the sampling capillary. The vacuum was used to pull a solution of 20 mM ascorbic acid through the capillary and the time required reach the detector recorded. From the time and the capillary volume the flow rate was calculated. The flow rates measured in this way were found to agree to within 5% with those predicted based on the Poiseuille equation ($n = 10$); therefore, for all further experiments the calculated values were used. The total volume of sample collected for an analysis was from 250-500 nL for samples collected at 1-10 nL/min and was 2.5 μL for sampled collected at 50 nL/min.

For simultaneous microdialysis-direct sampling experiments, a 3 mm side-by-side microdialysis probe built in-house (Church and Justice, 1987) was used. The microdialysis probes were perfused with aCSF at 70 nL/min allowing for a relative recovery of >97 % for all

analytes. Dialysate was monitored on-line using the same capillary electrophoresis system (see below) as described previously (Lada et al., 1997). The probe was implanted into the striatum to the same position as the direct sampling probe but in the contralateral striatum. Recordings were begun after the levels of target compounds reached a steady value, usually after 60 min. During the same time samples were collected from the direct sampling probe.

For some experiments dialysis probes were used to deliver agents to the tissue near the sampling probe inlet. For these experiments, the dialysis probe and direct sampling probe were glued together with a 200 μm gap between them. The direct sampling probe was positioned so that its tip aligned with the dorsal-ventral center of the dialysis probe. For these experiments, the dialysis probe was perfused at 1.2 $\mu\text{L}/\text{min}$ with either aCSF, 400 μM L-trans- pyrrolidine-2,4-dicarboxylic acid (PDC) in CSF, or high K^+ containing CSF. Initially, the dialysis probe was perfused with aCSF solution for 40 concurrent with direct sampling to establish baseline levels. At the end of this time a six-port valve (Model C6W, Valco, Houston TX) in line with the dialysis probe was manually switched such that a solution containing either the high K^+ or PDC could flow through the probe.

Sample Analysis. After completion of sample collection, the capillary was removed from the animal and mounted in the analytical system shown in Figure 1A. To perform the analysis, the syringe pump was used to drive sample and derivatization solution (37.5 mM o-phthaldehyde (OPA) and 71.5 mM β -mercaptoethanol (BME) in 20 mM borate buffer at pH 10.5) into a reaction capillary where the reagent and sample were allowed to mix and react to form fluorescent products. The resulting sample stream was then periodically injected onto the capillary electrophoresis column using the flow-gated interface.

The sampling capillary was mounted into the system as shown by the detail view in Figure 1B. The end of the sampling capillary nearest the experimental animal was threaded through two arms of a mixing tee (Valco, Houston, TX) and the inner bore of a 14 cm length of 360 μm O.D., 150 μm I.D. fused silica capillary which was also connected to the tee. The position of the sampling capillary was adjusted so that it was 6 cm from the end of the larger bore capillary. The larger bore capillary served as the derivatization reaction capillary and also transferred sample to the flow gate. Derivatization solution was pumped through the third arm of the tee so that the solutions could mix at the end of the sampling capillary. The sample and reagents were pumped at 50-166 nL/min for basal level measurements and 50 nL/min for monitoring applications. With these flow rates, the reagent and sample had over 60 s to react prior to injection on the electrophoresis capillary. This time is long enough for complete reaction (Lada et al., 1997). To initiate the analysis sequence, the valve shown in Figure 1A was switched from "off" position to "on" to allow the flow of sample into the reaction capillary. The collected sample was pumped out of the sampling capillary "last in-first out" and all temporal data shown are corrected for this inversion.

Capillary electrophoresis was performed using an in-house built instrument similar to that described previously (Lada et al., 1997). Electrophoretic separations were carried out using 10 μm I.D. by 360 μm O.D. fused silica capillaries with a total length of 7, 10, or 14 cm; however, the actual length used for separation was 3, 6, or 10 cm as the detection point was 4 cm from the outlet of the capillary. A Spellman 1000R CZE power supply (Plainview, NY) was used to supply 20 kV to the outlet of the column. Electrophoresis buffer consisted of 40 mM borate with 800 μM hydroxy-propyl β -cyclodextrin at pH 10.5. Sample was injected onto the separation capillary using the flow-gated interface as follows. During separations, electrophoresis buffer

was pumped through the flow-gate at 1.0 mL/min. This flow prevented sample from entering the electrophoresis capillary (see Figure 1B). To perform an injection, the separation voltage was turned off and an electrically-actuated valve (not depicted in the figure) used to stop gating-flow allowing sample to build-up in the flow-gate. After 5 s the injection voltage of 1 kV was applied for 600 ms in order to load sample onto the separation capillary. The injection voltage was then switched off and the gating valve opened to resume the gating flow. The voltage was then ramped up to 20 kV over the next 200 ms to initiate electrophoretic separation. All of these operations were performed automatically through a computer-controlled digital interface board (AT-MIO-16, National Instruments, Austin, TX) using software written in-house.

Electropherograms were recorded every 5-10 s until the sample capillary was emptied allowing determination of the analyte concentrations throughout the length of the separation capillary.

Detection of analyte zones was accomplished by laser-induced fluorescence (LIF). Forty mW of the 351 nm line of an argon-ion laser (Innova 300, Coherent, Santa Clara CA) was focused into the separation capillary. Fluorescence was collected at 90° from incident light through a 40x microscope objective (Melles Griot, Irvine, CA) passed through an iris, bandpass filter (S40-450, Corion, Holliston, MA) and focused onto a photomultiplier tube (R1477, Hamamatsu, Bridgewater, N.J.) biased at 900 V. Current generated at the photomultiplier tube was fed to a current amplifier (428 Current Amplifier, Keithley Instruments, Cleveland, OH) to convert to voltage for data acquisition. The current amplifier also provided a 30 ms rise time filter. Voltage out of the current amplifier was then sampled at 200-400 Hz using the same computer and board as was used for instrument control.

Data analysis. Analyte peaks were identified by comparing migration times in standards to those obtained from in vivo samples. Quantification of analytes was accomplished through

measurement of peak area for analytes and calibrated against standards. Peak areas were determined using statistical moments calculated by a data analysis program developed in-house. Statistical differences were evaluated by the Student's t-test.

Results

In Vitro Characterization of Direct Sampling. Initial experiments were conducted to investigate the feasibility of quantitatively sampling and analyzing nanoliter volume samples. In these experiments, sample was pulled from a vial into the sampling capillary by vacuum and pumped into the analysis system for read-out as described in the Methods section. The observed signal, measured as peak area for each separated compound, was plotted as a function of time in order to assess the temporal response as well as compare the signal intensity to standards. Figure 2 illustrates an example of such a plot as well as an individual electropherogram taken from the $t = 432$ s point of the read-out. The electropherogram illustrates the resolution of dopamine, γ -aminobutyric acid (GABA), taurine (TAU), glycine (GLY), glutamate (GLU) and aspartate (ASP) in the standard solution. The temporal response pattern of all analytes measured followed a similar trend to GLU and ASP but have been excluded from the graph for clarity. As expected, the plot of temporal response illustrates the peak areas are initially zero as the dead volume of the system is purged followed by a sharp increase as the sample capillary contents reach the electrophoresis capillary inlet. The peaks maintain a steady state area as the capillary is emptied and then declines during rinse out. The decline is not as sharp as the rise due to the laminar flow which causes dilution of the sample zone as it is pushed through the sample capillary. The relative standard deviation of the peak area for all analytes during steady state conditions for in vitro measurements was between 2.0-2.5%. More importantly, the peak areas in the electropherograms observed during the steady state region of the plot were within experimental

error (2-3%) of standards of identical concentration indicating the sample inside of the capillary can be quantitatively analyzed.

After completion of this initial characterization, the technique was applied to analysis of extracellular fluid (ECF) directly sampled from the striatum of an anesthetized rat. Figure 3 illustrates an electropherogram of the directly sampled ECF. Peaks corresponding to GABA, GLY, phosphoethanolamine (PEA), GLU and ASP have been identified and labeled. Dopamine and TAU could not be positively identified because of overlap with other peaks using these electrophoresis conditions. The temporal response to pumping the solution from the sampling capillary (Figure 3B) is nearly identical to that obtained for standards. The standard deviations of peak heights for in vivo analysis was 2.5 to 3.0% for all identified analytes during the steady state region of the plot.

Since samples are not filtered by a membrane and analysis occurs ~1-2 hours after initiation of sampling, it is possible that the sample may be prone to degradation by enzymes or other mechanisms which would lead to erroneous levels of transmitters. In order to assess the effect of sample degradation, experiments were conducted in which sample was collected at 10 nL/min and left in the sampling capillary at room temperature for 21 hours prior to analysis. At the end of this time the capillary contents were analyzed and results compared to results obtained for immediate analysis. The levels of transmitters determined immediately after sampling was 509 ± 103 , 247 ± 50 , 102 ± 22 , and 1910 ± 311 nM for GLU, ASP, GABA, and GLY respectively, while the levels observed after the delay was 466 ± 25 , 254 ± 74 , 99 ± 18 , 2010 ± 405 nM for GLU, ASP, GABA, and GLY respectively. Thus, no significant change in the sample occurred over the 21 hour time period indicating that degradation of the analytes was not appreciable over this time (n = 4).

Other possible problems associated with direct sampling such as clogging or interferences in the analysis due to proteins or particles were also not observed. In all of the experiments performed ($n = 35$), no clogging of the sampling capillary occurred. Interference from proteins was not observed in the analysis of the amino acids as illustrated by the electropherograms (Figure 3) which do not show loss of efficiency for the amino acids when compared to standards or significant broad peaks which would be expected for proteins in this system. It is possible that many proteins collected do not move through the capillary and are instead adsorbed to the sampling capillary thus preventing an effect on the analysis system.

Effect of Sampling Flow Rate on Analyte Levels. In direct sampling, it is possible that the rate of removal of extracellular fluid could affect the measurement; therefore, the effect of sampling flow rate in the range of 1-50 nL/min on the levels of transmitter was determined and results shown in Figure 4. A general trend of higher levels with lower sampling flow rates was observed; however, statistical significance of the difference was achieved only for the 1 and 2 nL/min samples compared to the 10 and 50 nL/min samples ($p < 0.05$ for all analytes). This result suggests that sampling at higher flow rates leads to analyte depletion in the vicinity of the sampling probe. This depletion apparently levels off at 1-2 nL/min as the analytes have similar levels at the two lower flow rates.

Comparison of Quantitative Microdialysis with Direct Sampling. To assess the quantification possible with direct sampling, results obtained with direct sampling at 1 nL/min were compared to dialysis measurements obtained in the contralateral striatum of the same rats. For these measurements, microdialysis was performed at 70 nL/min which gives a relative recovery $>97\%$ for all analytes and is expected to give quantitative recovery in vivo (Cosford et al., 1996; Lada and Kennedy, 1996). As shown in Figure 5, the levels of GABA, GLY, and

GLU were the same as measured by both low-flow rate microdialysis and low-flow direct sampling; however, ASP was significantly higher while PEA was significantly lower in the directly sampled fluid when compared to microdialysis.

Dynamic Monitoring with Direct Sampling. The direct sampling method was also used to assess concentration changes that occur during pharmacological treatments. In direct sampling as used here, concentration changes that occur during sampling are stored as concentration gradients within the 2 m long sampling tube so that temporal concentration information is stored along the length of the capillary. If the contents of the sampling capillary tube are pumped into the derivatization and analysis system at the same flow rate at which the sample was collected, then the electropherograms that are recorded represent analysis of samples collected at different times. Figure 6 illustrates the result of an *in vitro* experiment in which the concentration at the inlet of the sampling probe was changed from 1→10 μM of GLU and ASP at 17.5 min and then from 10→1 μM of GLU and ASP at 27.5 min and then analyzed as described above. As shown, the electrophoretic data record this change with a temporal resolution, defined as the time required for a step change in concentration to be recorded, of 45-90 s. The temporal resolution is limited by broadening of concentration pulses that occur due to flow and diffusion along the length of the capillary from the time of sampling until analysis.

To assess concentration changes *in vivo*, a microdialysis probe was implanted adjacent to the direct sampling probe and used to deliver agents to the region around the direct probe. When aCSF with 120 mM K^+ was perfused through the probe for 10 min the levels of glutamate and aspartate increased with a peak at 615 ± 95 and 542 ± 96 % of baseline respectively ($n = 4$). A sample trace of a K^+ stimulation is shown in Figure 7A. The time course data shows a typical latency of about 1 min between the time the high K^+ reached the microdialysis probe and

increases in amino acids were detected. Perfusing the dialysis probe with 400 μM of the GLU uptake inhibitor PDC evoked an average increase of $622 \pm 234 \%$ for GLU and $672 \pm 218 \%$ for ASP ($n = 5$). The sample time course data shown in Figure 7B shows a similar latency before the amino acids increase.

Discussion

Quantification of Neurotransmitters in ECF and Comparison to Microdialysis. One goal of this work was to determine if extracellular levels of neuroactive compounds could be quantified using a direct sampling approach. When fluid is removed at 10-50 nL/min, the measured levels of the neurotransmitters are lower than those found at the lower sampling rates. This result suggests that at higher sampling rates depletion of these compounds occurs in the vicinity of the sampling probe. To achieve an accurate measurement of the levels of transmitters in vivo it is necessary to sample such that the mass removal rate is less than the rate of release of transmitter into the extracellular space. Depletion of analytes at higher flow rates indicates that the analytes are not released and/or synthesized at a rate high enough to maintain the normal basal concentration. The origin of the extracellular component of the amino acid neurotransmitters is unclear making it problematic to predict the maximal rate of replenishment of neurotransmitters to the ECF and hence an appropriate sampling flow rate. The situation is complicated by the presence of high affinity uptake mechanisms in vivo which limit the distance transmitters can diffuse through the tissue. Furthermore, sampling may deplete ECF components, such as Ca^{2+} , altering normal brain function. However, our data indicate that comparable results are achieved when sampling at 1 or 2 nL/min for all analytes indicating that at these flow rates depletion no longer occurs. This result suggests that at these flow rates quantitative analysis of the ECF should be possible.

To assess whether the direct sampling method at 1 nL/min yielded a quantitative result, the results for sampling at this flow rate were compared to those for microdialysis sampling. In vivo calibration of microdialysis was achieved by operation at low flow rates. As seen in Figure 5, these two methods gave nearly identical results for GABA, GLY, and GLU suggesting that a quantitative measurement of these compounds is achieved by direct sampling. Quantitative measurements in this case refer to obtaining a spatially and temporally averaged measurement of the concentration in the extracellular fluid.

Although the low-flow rate microdialysis and direct sampling measurements for GABA, GLY, and GLU gave similar results, differences were noted for PEA and ASP. PEA concentrations recorded by low flow rate microdialysis were much higher than those measured by direct sampling. PEA levels have been suggested to be a sensitive indicator of membrane disruption after brain insult (Uchiyama-Tsuyuki et al., 1994). Thus, it is possible that the higher PEA levels in microdialysis samples reflect a greater degree of tissue damage associated with implantation of the larger microdialysis probe. A higher level of PEA may also result in microdialysis because of the way in which sample is collected. In microdialysis sample is collected through the sides of the probe meaning that it must come from tissue that has been penetrated, and therefore damaged, by the probe. In contrast, the direct sampling probe samples from just below the probe tip and therefore from tissue that has not been penetrated by the capillary. Therefore, it may be expected that smaller effects of membrane damage may be evident by direct sampling.

The ASP levels recorded by the dialysis probe and direct sampling probe were also different with a considerably higher level found in directly sampled fluid. The extracellular level of ASP (like GLU) under basal conditions does not decrease in response to local infusion of TTX

or depletion of Ca^{2+} suggesting that it does not derive directly from neuronal release (Herrera-Marschitz et al., 1996). Given that the origin of ASP is unknown, it is difficult to speculate on the cause of the discrepancy of ASP found in direct samples and dialysate. It is interesting in this regard however that regulation of ASP has been found to differ from GLU in the striatum under some conditions (Herrera-Marschitz et al., 1996; Lada et al., 1998).

Tissue Damage associated with Direct sampling. It is desirable that the sampling methods used for monitoring ECF minimize damage to the tissue being studied. Thus, microdialysis is favored over push-pull perfusion because it is perceived to have a lower impact on brain tissue. It is therefore of interest to assess the tissue damage associated with the direct sampling approach. Several lines of evidence support the notion that tissue damage associated with direct sampling is relatively small over the time course of measurements performed here. The lack of plugging of the sampling probes indicates that large amounts of debris were not created which would clog the sampling capillary. This conclusion is supported by visual inspection of the ECF collected at 1-50 nL/min which revealed a clear fluid with no particulates whereas samples collected by push-pull perfusion contain numerous particles of cellular debris and are tinged with red suggesting rupture of blood vessels. The observation that the concentrations of the amino acids remained steady over the course of data collection (see Figures 3 and 7) also supports the idea that continuous sampling does not create acute changes associated with tissue damage. As mentioned above, the lower PEA levels also support the idea of minimal local tissue damage. Finally, preliminary histological examinations of the tract near the direct sampling probe revealed no obvious cell damage 5 μm below the tip of the probe although an absence of cells was observed immediately below the tip of the probe. While a more complete histological examination is required to fully determine the tissue damage associated with the

direct sampling probe; the observations obtained so far are supportive of disruption of tissues that is much less than push-pull perfusion and not greater than microdialysis.

Spatial Resolution of Direct Sampling. The direct sampling probe is quite small compared to the active area of microdialysis probes suggesting that a potential advantage of direct sampling over microdialysis would be better spatial resolution. The spatial resolution of direct sampling will depend on the sampling flow rate and transport kinetics of the transmitter of interest. If spatial resolution is defined as a sphere within which a molecule has > 50% chance of being collected by the direct sampling probe, then the spatial resolution can be estimated by:

$$R_{\text{spat}} = (t_{1/2}) (q) (1/\chi)$$

where (R_{spat}) is the spatial resolution in cm^3 , $t_{1/2}$ is the average half life of a transmitter molecule in the ECF in seconds, q is the sampling flow rate (mL/s) and χ is the extracellular volume fraction ($\chi = 0.2$). The half-life of a transmitter molecule can be estimated using Michaelis-Menton kinetics for the clearance of the transmitter from the ECF. Using previously published values for K_m and V_{max} for the glutamate transporter (Erecinska and Silver, 1990) we estimate the glutamate sampled in our experiments represents that within a sphere of radius between 30 and 80 μm . The large range for the spatial resolution with respect to GLU is due to the wide range of values reported for K_m and V_{max} of the GLU transporter. This spatial resolution will allow measurements in small brain nuclei not experimentally accessible by dialysis. The high level of spatial resolution obtained may also allow observation of concentration gradients within the tissue which have previously been observed using through microelectrodes (Kawagoe et al., 1992).

Monitoring Changes in GLU and ASP. The direct sampling technique was also evaluated for monitoring dynamic changes in neurotransmitter concentration. With a depolarizing agent

(120 mM K^+) or uptake inhibitor (PDC) applied through an adjacent microdialysis probe, reproducible increases in GLU and ASP with a magnitude similar to those observed by microdialysis were detected (Figure 7). A slight delay was observed between the time that the K^+ or PDC reached the dialysis probe and detection of an increase in the excitatory amino acids. This delay likely represents the time required for the effective concentrations of these agents to reach the neurons sampled by the direct sampling probe. Combined, these data illustrate that the direct sampling probe can detect changes in concentration in vivo and can sample active tissue much like microdialysis.

Conclusions. Direct sampling at 1-50 nL/min appears to be a viable method for accessing the extracellular fluid of the brain in living animals. Measurements of neuroactive substances yields results that are in general similar to calibrated microdialysis measurements when sampling rates at 1-2 nL/min are used. The ability to observe changes in response to depolarizing agents and uptake inhibitors demonstrates the ability to record dynamic changes and to sample from active neurons. The technique produces only nanoliter samples; however, by storage in the capillary and analysis with an on-line capillary electrophoresis system, these small samples are readily manipulated and analyzed. Although analysis was performed immediately after collection, it may be possible to freeze the sample in the capillary and analyze at a later time. Furthermore, it may be possible to improve the system by developing microscale pumps to remove sample for continuous on-line analysis. This development would permit longer term measurements than those achieved here by storing sample in the sampling capillary. In principle, the method is fully compatible with freely moving animals; however, this has yet to be demonstrated. Compared with microdialysis, the primary advantage of the direct sampling approach appears to be significantly higher spatial resolution. Such higher spatial resolution

should allow studies in previously inaccessible nuclei and studies on heterogeneity in larger brain structures. Issues to be addressed with regard to direct sampling include more thorough evaluation of tissue damage caused by the probes and sources of quantitative differences between this method and microdialysis for analytes such as ASP.

Acknowledgements. This work was supported by NIH (NS38476). We thank Dr. Michael T. Bowser for helpful discussions.

Figure Legends

Figure 1. (A) Diagram of the flow-gated capillary electrophoresis instrument used for analysis of directly sampled ECF. HV is the high voltage lead. (B) Diagram of the flow gated interface and associated capillaries enlarged for clarity. The sampling capillary is threaded into the large bore reaction capillary so as to create a zero dead volume connection. Derivatization reagents are pumped into the tee and between the sampling capillary and larger bore reaction capillary. The derivatized amino acids were introduced onto the electrophoresis column through the flow-gated interface as described in the text.

Figure 2. (A) Capillary electrophoresis separation of standards of 1.5 μM dopamine, 3 μM GABA, 2 μM TAU, 0.7 μM GLY, 1.5 μM GLU, and 0.8 μM ASP taken at point $t = 432$ s from the plot in Figure 2B. Electrophoresis capillary was 10 cm long (injection to detection point). (B) Temporal response pattern observed as sample is readout into the analysis system. Each data point is the peak area taken from a single electropherogram. The time between the start of the trace and the first increase is due to the dead volume of the system. The signal reaches a steady state value representing transmitter levels in the sample prior to declining as the collected sample is completely washed out and diluted by aCSF which is being pumped through the capillary behind the plug of sample.

Figure 3. (A) Electropherogram of directly sampled ECF collected at 10 nL/min from the rat striatum. Peaks corresponding to GABA, GLY, PEA, GLU and ASP are labeled. (B) Plot demonstrating the typical response seen over the course of washout of the ECF from the sampling capillary for GLU and ASP.

Figure 4. Effect of sampling flow rate on concentration of analytes detected by capillary electrophoresis-LIF in ECF. Plot is shown on a log-log axis because of the large difference in

concentrations for the different analytes. Error bars are ± 1 standard error of the mean ($n = 8$ for 1 and 2 nL/min and $n = 5$ for 10 and 50 nL/min). All measurements were from different animals. The levels recorded from samples collected at 10 and 50 nL/min were significantly lower than those recorded at 1 and 2 nL/min for all analytes ($p < 0.05$).

Figure 5. Comparison of analyte levels determined in striatum using low-flow microdialysis (70 nL/min) and direct sampling (1 nL/min). The microdialysis flow rate is low enough to give relative recovery $>97\%$ for all analytes and is therefore considered to give quantitative recovery. Asterisks (*) denote that levels observed through microdialysis and direct sampling are statistically different ($p < 0.05$). Error bars represent ± 1 standard error of the mean ($n = 4$).

Figure 6. Test of the temporal response of the direct sampling system. Sample was collected from a vial at 50 nL/min into a 200 long 40 μm i.d. capillary for 40 min. Sample contained 1.5 μM GLU and 0.8 μM ASP. From 17.5 to 27.5 min the concentration in the vial was changed to 10 μM GLU and 5 μM ASP. Plot shows the peak areas for GLU and ASP recorded as the sampling capillary was pumped into the analysis system at 50 nL/min. Each point is the peak area from one electropherogram. The figure illustrates monitoring changes in ECF transmitter concentrations is possible with temporal resolution of < 90 seconds.

Figure 7. Detection of dynamic changes in vivo by direct sampling. A dialysis probe and direct sampling capillary were implanted into the striatum with a 200 μm gap between them. The probe was used to deliver 120 mM K^+ (A) or 400 μM of the GLU uptake inhibitor PDC (B) as ECF was collected by the direct sampling probe. Bars indicate application of the stimulus through the probe. Samples were collected at 50 nL/min and pumped into the analytical system at the same rate. Each point is the peak area from one electropherogram. The electrophoresis

capillary was 3 cm long (injector to detector). Under these conditions only GLU and ASP are resolved. Data is representative from 4 experiments for the K^+ stimulation and 5 experiments for PDC treatment.

References

- Benveniste H. Brain microdialysis. *J. Neurochem.*, 1989; 52: 1667-1679.
- Boyd BW, Witowski SR, Kennedy RT. Trace-level amino acid analysis by capillary liquid chromatography and application to in vivo microdialysis sampling with 10-s temporal resolution. *Anal. Chem.*, 2001; 72: 865-871.
- Bungay PM, Detrick RL, Fox E, Balis FM. Probe calibration in transient microdialysis in vivo. *Pharm. Res.*, 2001; 18: 361-366.
- Burmeister JJ, Gerhardt GA. Self-referencing ceramic-based multisite microelectrodes for the detection and elimination of interferences from the measurement of L-glutamate and other analytes. *Anal. Chem.*, 2001; 73: 1037-1042.
- Chen A, Lunte, CE. Microdialysis sampling coupled on-line to fast microbore liquid chromatography. *J Chromatogr A.*, 1995; 691: 29-35
- Church W, Justice, JB Jr. Rapid sampling and determination of extracellular dopamine in vivo. *Anal Chem.*, 1987; 59: 712-716.
- Cosford RJ, Vinson AP, Kukoyi S, Justice JB Jr. Quantitative microdialysis of serotonin and norepinephrine: pharmacological influences on in vivo extraction fraction. *J. Neurosci. Meth.*, 1996; 68: 39-47.
- Erecinska M, Silver IA. Metabolism and role of glutamate in mammalian brain, *Prog. Neurobiol.*, 1990; 35: 245-296.
- Gaddum JH. Push-pull cannulae, *J. Physiol.* 1961; 155: 1P.
- Georganopoulou DG, Carley R, Jones DA, Boutelle MG. Development and comparison of biosensors for in-vivo applications. *Faraday Discuss.* 2000; 116: 291-303.
- Herrera-Marschitz M, You ZB, Goiny M, Meana JJ, Silveira R, Godukhin OV, Chen Y, Espinoza S, Pettersson E, Loidl CF, Lubec G, Andersson K, Nylander I, Terenius L, Ungerstedt U. On the origin of extracellular glutamate levels monitored in the basal ganglia of the rat by in vivo microdialysis. *J. Neurochem.*, 1996; 66: 1726-1735.
- Izquierdo I, Izquierdo J. Effects of drugs on deep brain centers. *Ann. Rev. Pharmac.*, 1971; 11: 189-208.
- Justice JB Jr. Quantitative microdialysis of neurotransmitters. *J. Neurosci. Methods*, 1993; 48: 263-276.
- Kawagoe KT, Garris PA, Wiedemann DJ, Wightman RM. Regulation of transient dopamine concentration gradients in the microenvironment surrounding nerve terminals in the rat striatum. *Neuroscience*, 1992; 51: 55-64.

Kissinger PT. Microdialysis and liquid chromatography. In Robinson TE, Justice JB Jr. editors. *Techniques in the Behavioral and Neural Sciences: Microdialysis in the Neurosciences*. Elsevier: Amsterdam, 1991; 7: 103-116.

Kulagina NV, Shankar L, Michael AC. Monitoring glutamate and ascorbate in the extracellular space of brain tissue with electrochemical microsensors. *Anal. Chem.*, 1999; 71: 5093-5100.

Lada MW, Kennedy RT. Quantitative in vivo monitoring of primary amines in rat caudate nucleus using microdialysis coupled by a flow-gated interface to capillary electrophoresis with laser-induced fluorescence detection. *Anal. Chem.*, 1996; 68: 2790-2797.

Lada MW, Vickroy TW, Kennedy RT. High temporal resolution monitoring of glutamate and aspartate in vivo using microdialysis on-line with capillary electrophoresis with laser induced fluorescence detection. *Anal. Chem.*, 1997; 69: 4560-4565.

Lada, MW, Vickroy TW, Kennedy RT. Evidence for neuronal origin and metabotropic Receptor-mediated regulation of extracellular glutamate and aspartate in rat striatum in vivo following electrical stimulation of the prefrontal cortex. *J. Neurochem.*, 1998; 70: 617-625.

Lerma J, Herranz AS, Abaira V, Martin Del Rio R. In vivo determination of extracellular concentration of amino acids in the rat hippocampus-a method based on brain dialysis and computerized analysis. *Brain Res.*, 1986; 384: 145-155.

Lonnroth P, Jansson PA, Smith U. A microdialysis method allowing characterization of intercellular water space in humans. *Am. J. Physiol.*, 1987; 253: E228-E231.

Marsden CD, Martin KF, Routledge C, Brazell MP, Maidment NT. Application of intracerebral dialysis and in vivo voltammetry to pharmacological and physiological studies of amine neurotransmitters. *Ann. NY Acad. Sci.*, 1986; 473: 106-125.

Myers RD. Methods for perfusing different brain structures. In Myers RD, editor. *Methods in Psychobiology*, Academic Press: London, 1972; 2: 169-211.

Parsons LH, Smith AD, Justice JB Jr. Basal extracellular dopamine is decreased in the rat nucleus accumbens during abstinence from chronic cocaine. *Synapse*, 1991; 9: 60-65.

Peters JL, Michael AC. Modeling voltammetry and microdialysis of striatal extracellular dopamine: the impact of dopamine uptake on extraction and recovery ratios. *J. Neurochem.*, 1998; 70: 594-603.

Robert F, Bert L, Parrot S, Denoroy L, Stoppini L, Renaud B. Coupling on-Line brain microdialysis, precolumn derivatization and capillary electrophoresis for routine minute sampling of *o*-phosphoethanolamine and excitatory amino acids. *J. Chromatogr. A*, 1998; 817: 195-203.

Tucci S, Rada P, Sepulveda MJ, Hernandez L. Glutamate measured by 6-s resolution brain microdialysis: capillary electrophoretic and laser-induced fluorescence detection application. *J. Chromatogr. B*, 1997; 694: 343-349.

Uchiyama-Tsuyuki Y, Araki H, Yae T, Otomo S. Changes in the extracellular concentrations of amino-acids in the rat striatum during transient focal cerebral ischemia. *J. Neurochem.*, 1994; 62: 1074-1078.

Ungerstedt U, Hallstrom A. In vivo microdialysis--a new approach to the analysis of neurotransmitters in the brain. *Life Sci.*, 1987; 41: 861-864.

Ungerstedt U. Introduction to microdialysis. In Robinson TE, Justice JB Jr. editors. *Techniques in the Behavioral and Neural Sciences: Microdialysis in the Neurosciences*, Elsevier: Amsterdam, 1991; 7: 3-18.

Wages SA, Church WH, Justice JB Jr. Sampling considerations for on-line microbore liquid chromatography of brain dialysate. *Anal. Chem.*, 1986; 58: 1649-1656.

Zhou SY, Zuo H, Stobaugh JF, Lunte CE, Lunte SM. Continuous in vivo monitoring of amino acid neurotransmitters by microdialysis sampling with on-line derivatization and capillary electrophoresis separation. *Anal Chem.*, 1995; 67: 594-599.

Zoli M, Torri C, Ferrari R, Jansson A, Zini I, Fuxe K, Agnati LF. The Emergence of the volume transmission concept. *Brain Res. Rev.*, 1998; 26: 136-147.

Fig 1

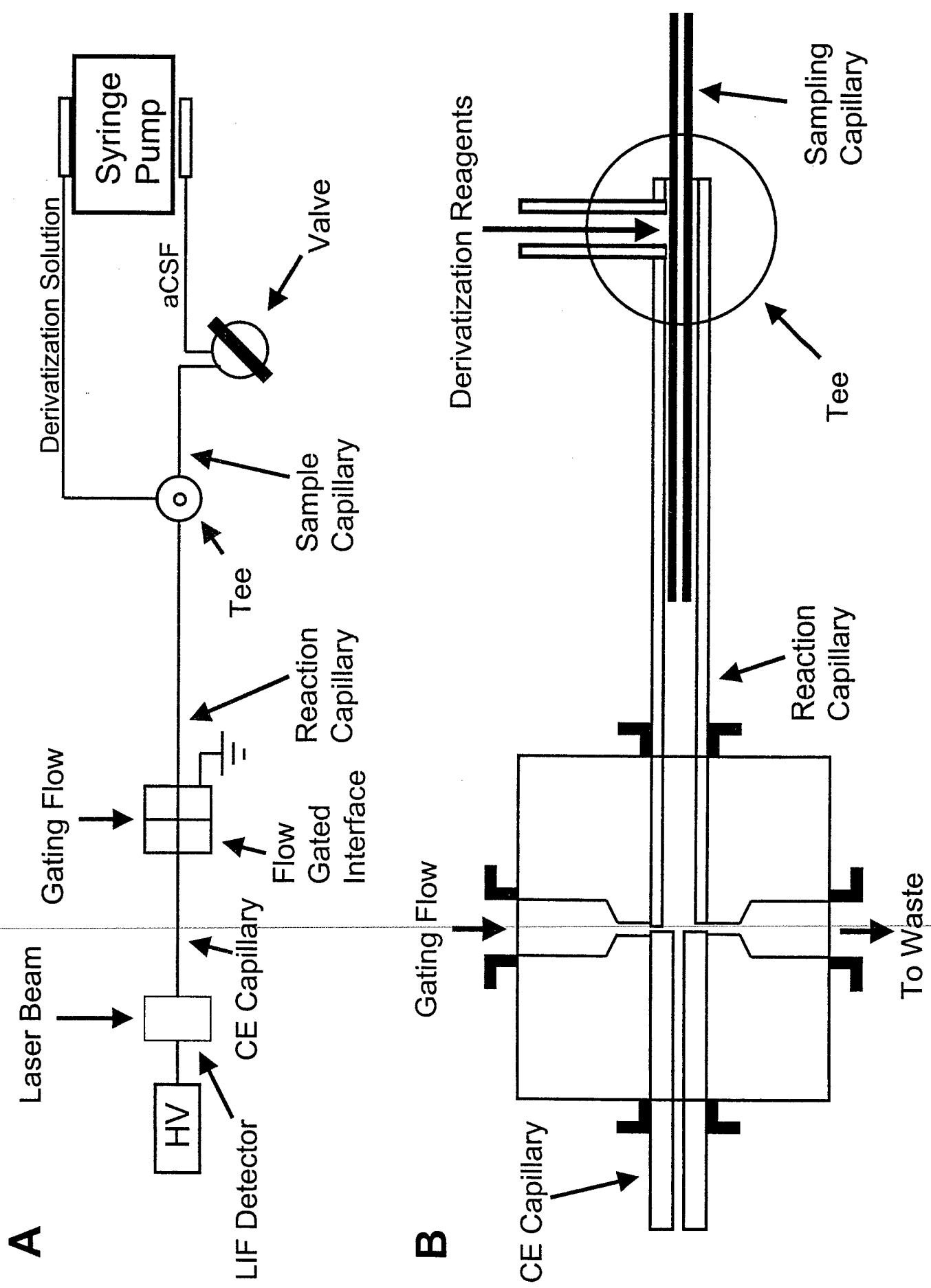


Fig 2

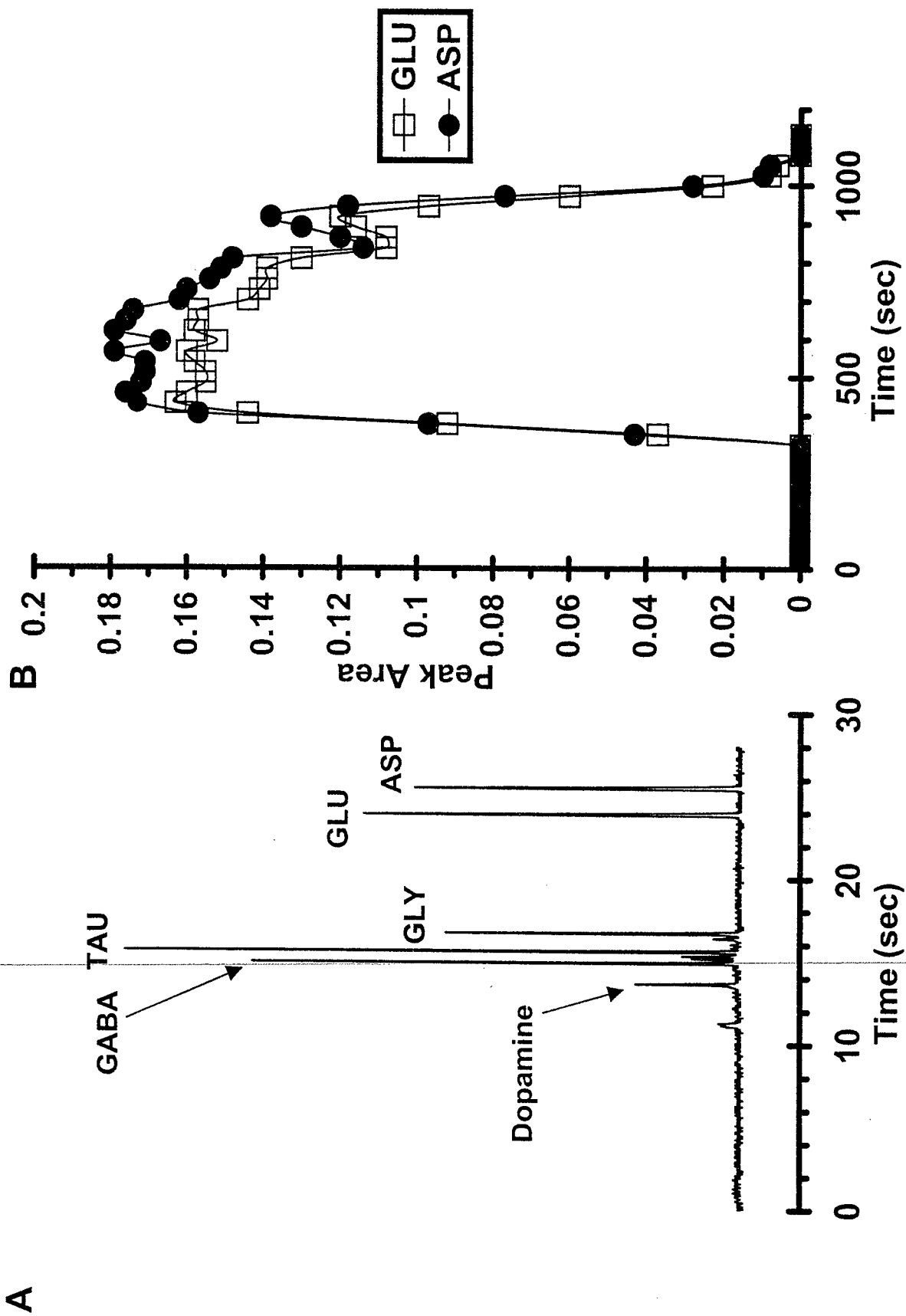


Fig 3

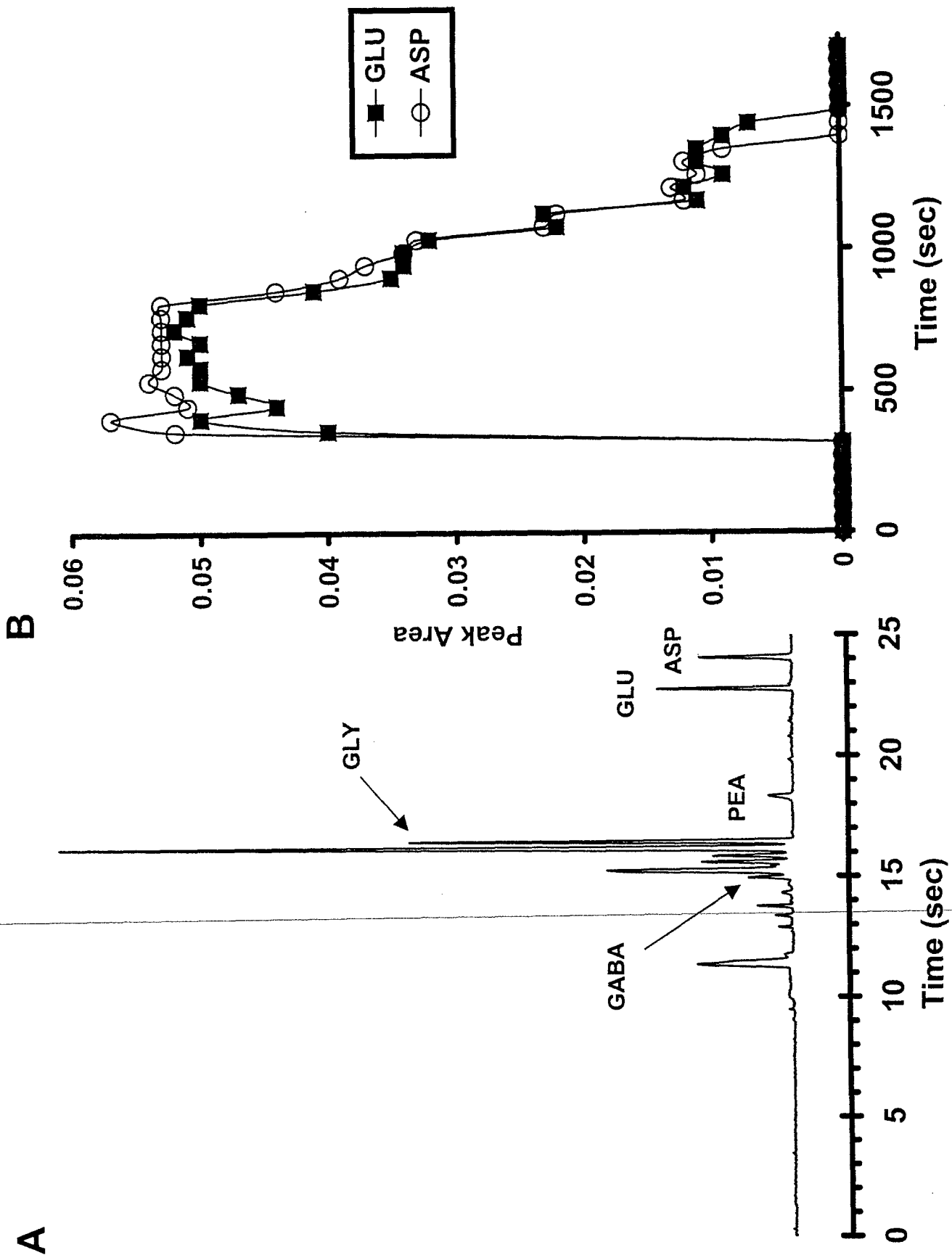


Fig 4

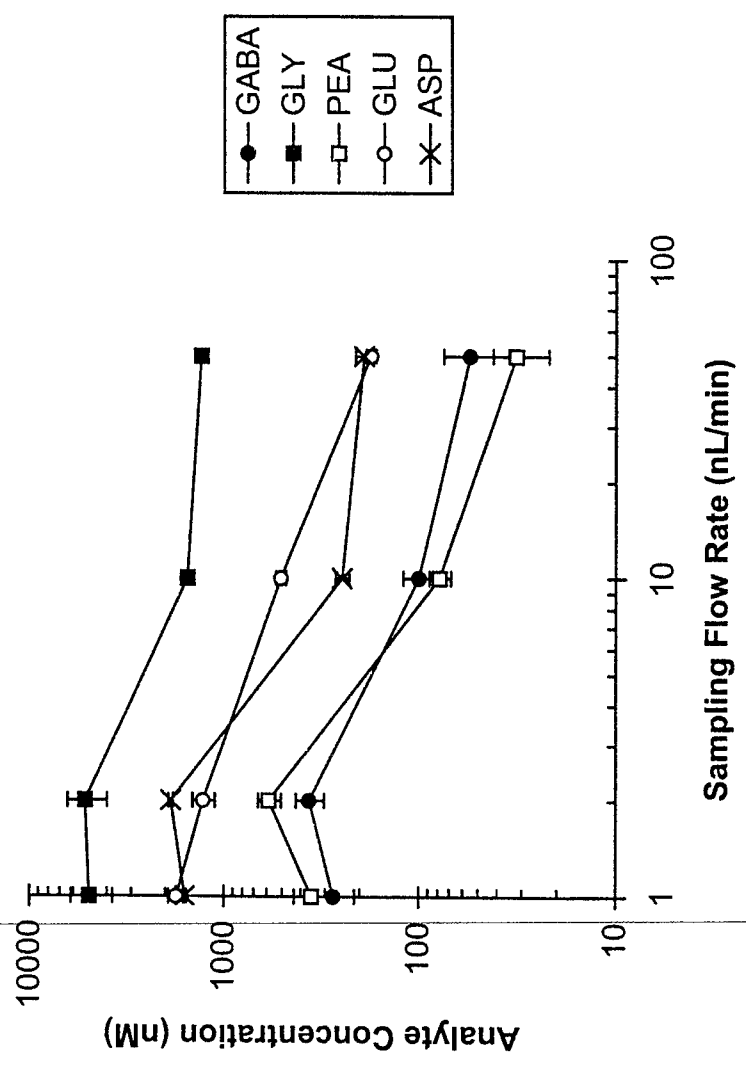


Fig 5

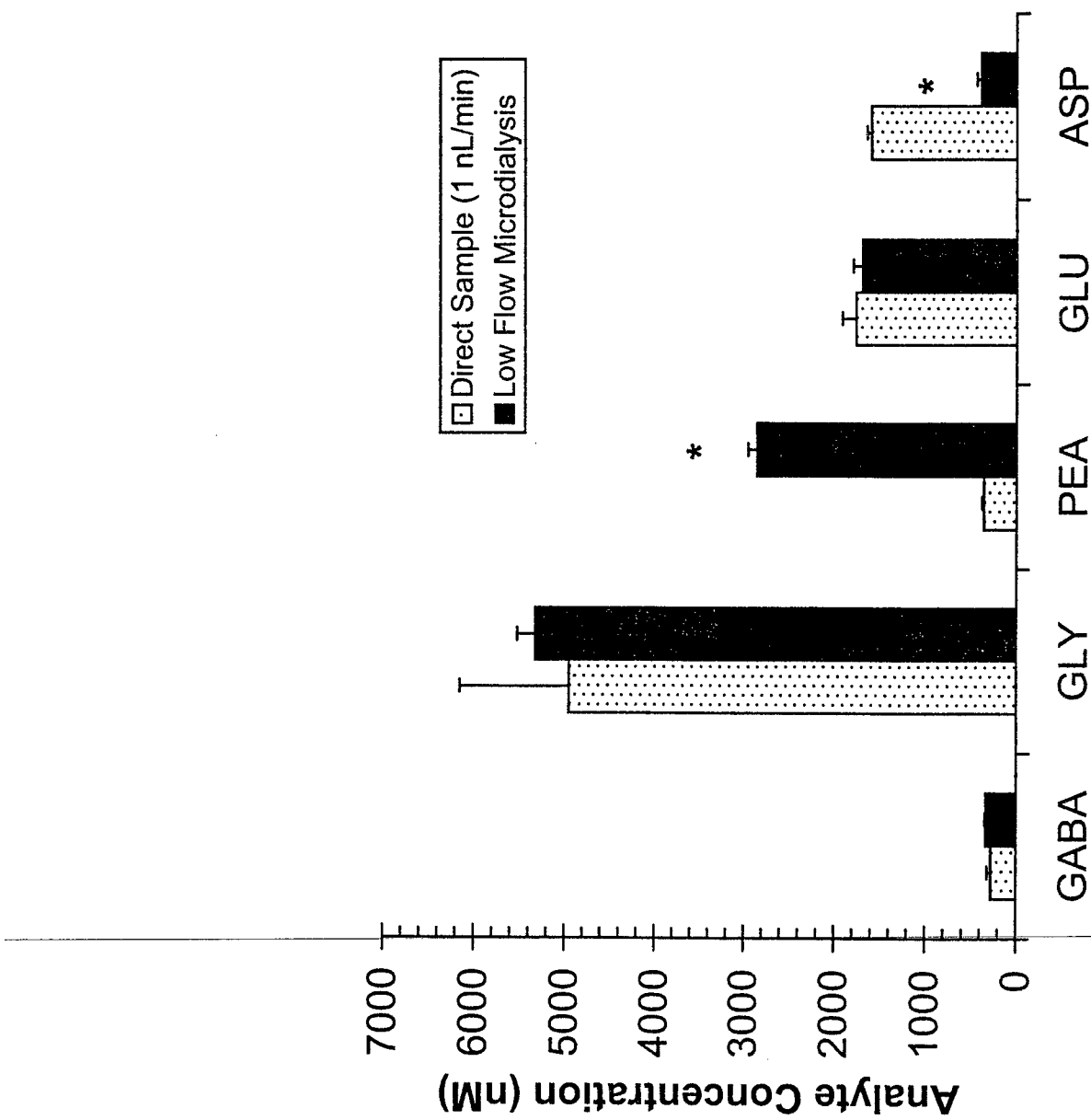


Fig 6

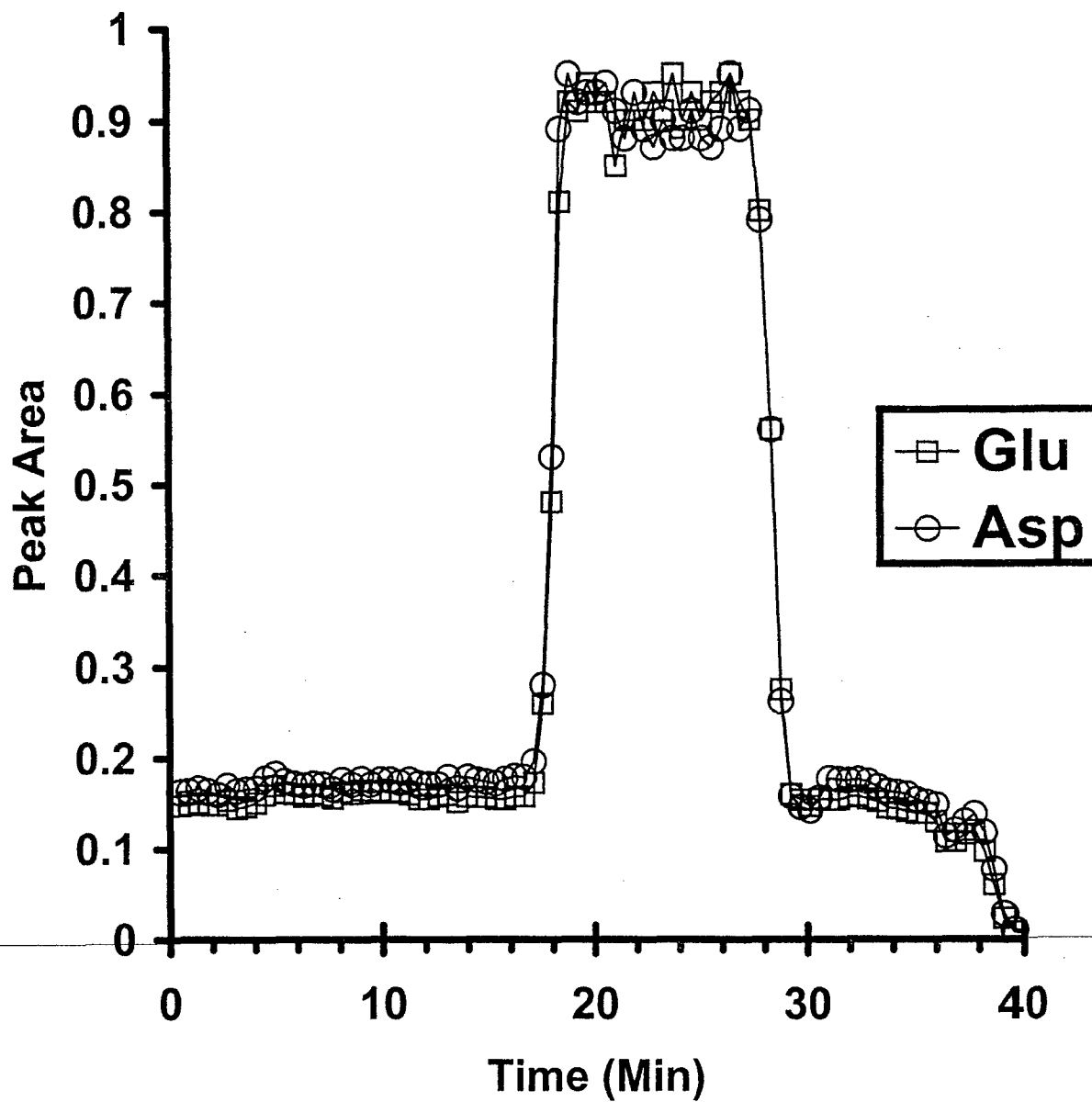
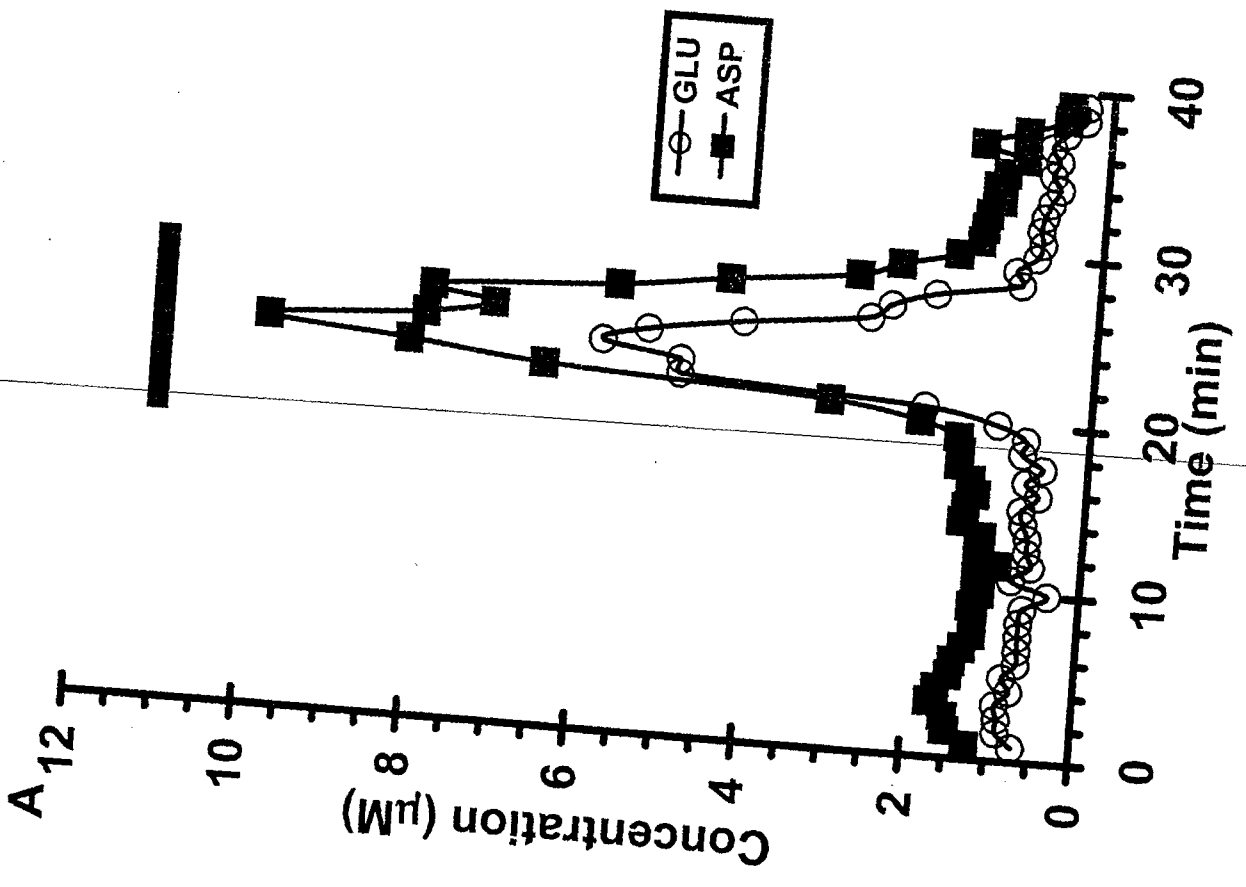
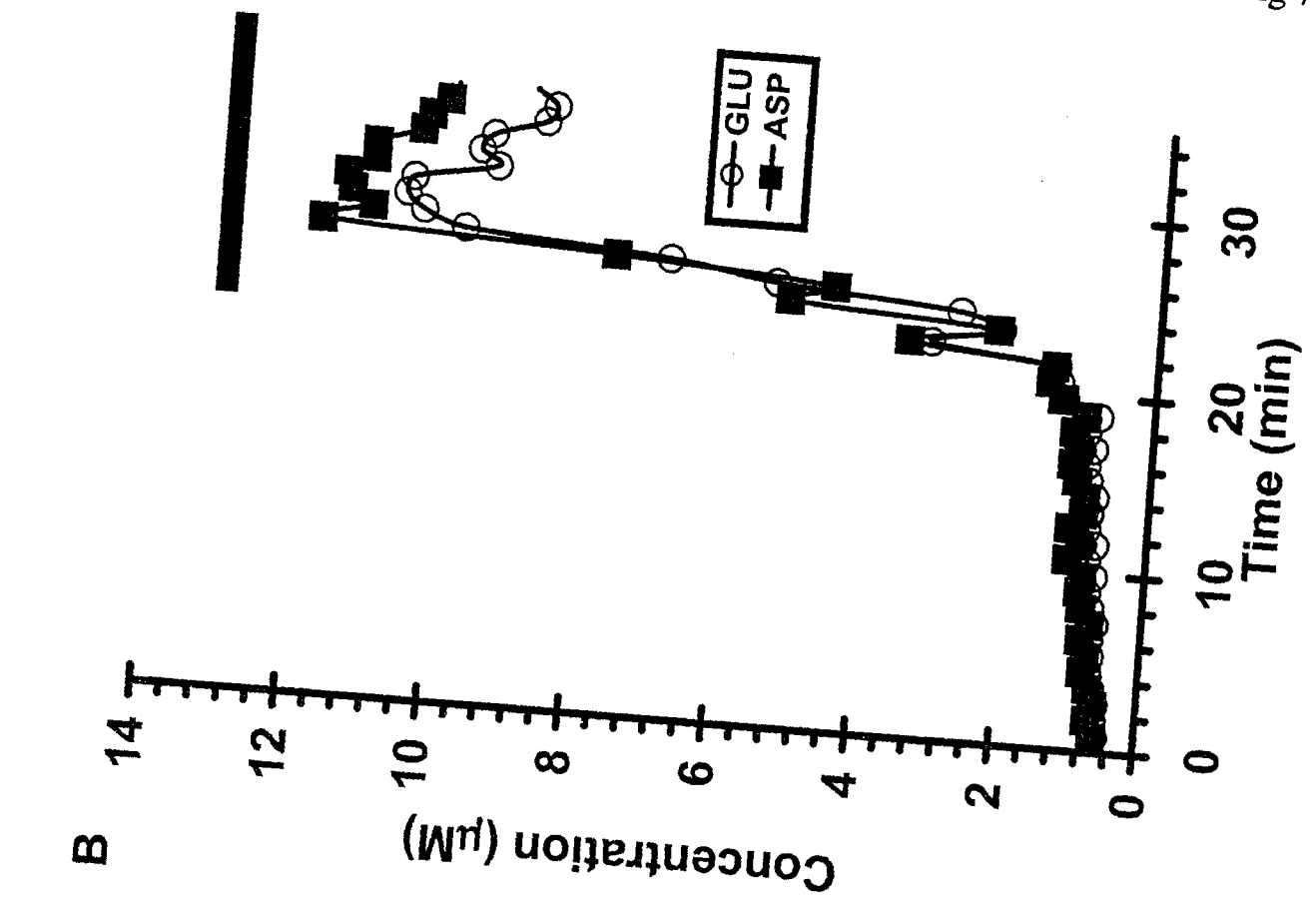


Fig 7





DEPARTMENT OF THE ARMY
US ARMY MEDICAL RESEARCH AND MATERIEL COMMAND
504 SCOTT STREET
FORT DETRICK, MARYLAND 21702-5012

REPLY TO
ATTENTION OF:

MCMR-RMI-S (70-1y)

28 Aug 02

MEMORANDUM FOR Administrator, Defense Technical Information
Center (DTIC-OCA), 8725 John J. Kingman Road, Fort Belvoir,
VA 22060-6218


SUBJECT: Request Change in Distribution Statement

1. The U.S. Army Medical Research and Materiel Command has reexamined the need for the limitation assigned to technical reports written for this Command. Request the limited distribution statement for the enclosed accession numbers be changed to "Approved for public release; distribution unlimited." These reports should be released to the National Technical Information Service.

2. Point of contact for this request is Ms. Kristin Morrow at DSN 343-7327 or by e-mail at Kristin.Morrow@det.amedd.army.mil.

FOR THE COMMANDER:

Encl


PHYLIS M. RINEHART
Deputy Chief of Staff for
Information Management

ADB231838
ADB240253
ADB251610
ADB275099
ADB253637
ADB261538
ADB275186
ADB264648
ADB275102
ADB241899
ADB259033
ADB266113
ADB275663
ADB254489
ADB262700
ADB276708
ADB274345
ADB274844
ADB275154
ADB275535
ADB275101
ADB275451
ADB274597
ADB273871
ADB275145
ADB274505
ADB275851
ADB274459
ADB277942
ADB277404
ADB277494
ADB277536